



JPRS Report

Science & Technology

China

DISTRIBUTION STATEMENT A
Approved for public release;
Distribution Unlimited

DEFO QUANTITY INSPECTED 1

19980115 033

Science & Technology China

JPRS-CST-93-010

CONTENTS

27 May 1993

SCIENCE & TECHNOLOGY POLICY

State Invests 5 Billion Yuan To Aid Science Research [Ma Zhiping; CHINA DAILY, 8 May 93]	1
New Group Formed To Promote High-Tech Exports [Wang Yong; CHINA DAILY, 17 May 93]	1
Government Officials Speak at World Telecommunications Day Symposium [Xie Liangjun; CHINA DAILY, 18 May 93]	2
Scientific Knowledge Profitable, Says Jiang Zemin [He Jun; CHINA DAILY, 15 May 93]	3

AEROSPACE

Development of China's Launch Vehicle Systems [Liu Yansheng; HANGTIAN, 26 Mar 93]	4
---	---

DEFENSE R&D

An Approach to Radar Target Recognition Using Wideband Millimeter-Wave Technology [He Songhua, Guo Guirong; HONGWAI YU HAOMIBO XUEBAO, No 6, Dec 92]	7
---	---

BIOTECHNOLOGY

Isolation and Characterization of a Human cDNA of Pro-Urokinase [Hu Meihao; BEIJING DAXUE XUEBAO, No 2, Mar 93]	11
Channel-Forming Activity of Yular Lipid Bilayer of the Membrane Active Polypeptide B Form Venom of Bungarus Fasciatus [Shi Yuliang, Wang Wenping, et al.; SHENGLI XUEBAO, No 6, Dec 92]	11
Design and CD Study of α/β Alterable Peptides [Xu Mei, Zhang Ying, et al.; SHENGWUHUAXUE YU SHENGWUWULI XUEBAO, No 4, Jul 92]	11
Synthesis of Insulin Analogues With Deletions at the Helical Region of the A Chain [Yang Shizhen, Huang Yiding, et al.; SHENGWUHUAXUE YU SHENGWUWULI XUEBAO, No 6, Nov 92]	11
Molecular Cloning and High Expression of Yeast PHO 85 Gene in E. coli [Zhong Hualin, Li Boliang, et al.; SHENGWUHUAXUE YU SHENGWUWULI XUEBAO, No 6, Nov 92]	11
The ^1H Resonance Assignment of Modifier of 16-Peptide Fragment in Rat TGF- α Using 2D NMR [Huang Yongren, Sheng Wanyun, et al.; SHENGWUHUAXUE YU SHENGWUWULI XUEBAO, No 6, Nov 92]	12
Synthesis of a Modified T ₅ P ₂₅ Promoter and Its Use for High-Level Expression of IFN- α A Gene [Wang Chengyao, Tang Jinyan, et al.; SHENGWUHUAXUE YU SHENGWUWULI XUEBAO, No 6, Nov 92]	12
PCR-Amplification, Cloning and Sequencing of 2F7 Monoclonal Antibody Variable Domains [Wu Wenshu, Huang Zhenyu, et al.; SHENGWUHUAXUE YU SHENGWUWULI XUEBAO, No 6, Nov 92]	12
Secretion of Overproduced Human Epidermal Growth Factor in Escherichia coli [Gan Renbao, Huang Peiyong, et al.; SHENGWUHUAXUE YU SHENGWUWULI XUEBAO, No 6, Nov 92]	12
2D-NMR Studies of α/β Alterable Peptides [Xu Mei, Xu Lingfei, et al.; SHENGWUHUAXUE YU SHENGWUWULI XUEBAO, Jan 93]	13
Solution Conformation Studies on Bradykinin by 2D-NMR and Molecular Dynamics [Yang Weiwen, Wang Sanshan, et al.; SHENGWUHUAXUE YU SHENGWUWULI XUEBAO, Jan 93]	13
In Vitro Inhibition of Indirect Immunotoxin Mediated by Monoclonal Antibody on Human Melanoma Cell Line [Zhang Zuchuan, Zhang Ruping, et al.; SHENGWUHUAXUE YU SHENGWUWULI XUEBAO, Jan 93]	13

Enhancement of Thermostability of Subtilisin E by Means of Protein Engineering
[Wang Xianshun, Wang Peizhi, et al.; SHENGWUHUAXUE YU SHENGWUWULI XUEBAO,
Jan 93] 13

COMPUTERS

Additional Details on 1992 High-Tech Import, Export Figures
[Liu Jiuru; JISUANJI SHIJIE, 21 Apr 93] 15

U.S. Firm AMNET Introduces Integrated WAN Technology to China
[Ying Zi; JISUANJI SHIJIE, 28 Apr 93] 15

Wanfang Markets China Enterprise, Corporation, and Product Database
[Liu Jing; JISUANJI SHIJIE, 28 Apr 93] 15

Design, Implementation of Knowledge-Based Operating Language
[Liao Minghong, Guo Fushun, et al.; XIAOXING WEIXING JISUANJI XITONG, Apr 93] 15

LASERS, SENSORS, OPTICS

Nation's First Satellite GPS Applications System Operational
[Yuan Wen; RENMIN RIBAO OVERSEAS EDITION, 5 May 93] 17

Utilitarian DAT Player, 5.25-Inch Erasable Rewritable Magneto-Optical Disk Unveiled
[Yu Zhuo, Zhou Ganpu; KEJI RIBAO, 26 Apr 93] 17

Experimental Research on Ultrafine (Nanoscale) Optoelectronic-Conversion Thin Film
[Wu Jinlei, Liu Weimin, et al.; KEXUE TONGBAO, 1-15 Feb 93] 17

Optical Implementation of Perfect Shuffle/Exchange Omega Interconnection Network
[Cao Mingcui, Li Hongpu, et al.; GUANGXUE XUEBAO, Dec 92] 19

Carrier-Injected GaAs/GaAlAs Total Internal Reflection Optical Switch
[Zhuang Wanru, Lin Wenhua, et al.; BANDAOTI XUEBAO, Jan 93] 23

State Invests 5 Billion Yuan To Aid Science Research

40101013A Beijing CHINA DAILY in English
8 May 93 p 1

[Article by staff reporter Ma Zhiping]

[Text] Noting that technological inventions have brought considerable economic benefits to China, the State revealed yesterday it invested 5 billion yuan (\$900 million) to support the application of more than 500 new State-level scientific innovations during the past 4 years.

The announcement was made in Beijing by officials with the State Commission for Science and Technology, the bureau that initiated the drive for new science and technology in 1989.

For the industrial sector alone, more than 200 advanced technologies have been put into use in about 3,700 enterprises, producing 48 billion yuan (\$800 million) in extra earning and 100 billion yuan (\$16.7 billion) in industrial output value, commission members said.

Agriculture has been a prime beneficiary of new technologies, officials added.

"Coupled with the technical renovation of production in industrial enterprises, new scientific findings in the agricultural field have played a very important role and achieved much greater benefits in developing a high quality and efficient agricultural system. These have enhanced the technical advancement of rural enterprises in China," said the official in charge of the management of new science and technology achievements.

He said 112 advanced technologies have produced an output value of 100 million yuan (\$16.7 million) in the industrial and agricultural aspects during the past 4 years.

For example, the sparse planting of uplands rice, a new State-level farming technology, is making an annual economic benefit of 2 billion yuan (\$330 million). Two-thirds of the rice-growing areas in north China are using the invention, which is now being promoted in the southern parts of the country, as well.

"The ratio of increased farm yield from using new technology is growing from about 20 percent several years ago to the present 35 percent, a figure indicating the importance of the science and technology application programme," said officials with the State Science Commission.

Since 1989, more than two million scientific workers have devoted themselves to the promotion of the new technologies programme, whose implementation has brought about the formation of nationwide systems and networks for scientific promotion.

To date, over 220,000 science promotion teams have emerged across the country for the application of new agricultural and forestry production technologies and

about 40 provinces, autonomous regions and cities have worked out their own local promotion plans, according to the commission's spokesman.

"We will attach more importance to the combination of macro-leadership and guidance with market mechanism in the promotion of new technologies this year and in following years," noted officials at the briefing.

They added the adoption of a market mechanism has considerably enhanced the spread of new technologies in recent years.

Last year, Chinese scientists made over 35,400 scientific innovations, among which 10,900 won provincial and ministry-level awards, and 5,200 findings reached the advanced international level.

New Group Formed To Promote High-Tech Exports

40101013B Beijing CHINA DAILY [BUSINESS WEEKLY] in English 17 May 93 pp 1-2

[Article by Wang Yong]

[Text] China's largest technology trading company will sign up major Chinese high-tech units to form a high-powered conglomerate this year.

Tong Changyin, president of the China National Technology Import and Export Corporation (CNTIC), described the move as its trump card in gearing up the country's hi-tech exports.

The envisioned group will unleash China's hi-tech development capacity as high-profile results will find easier access to the markets.

In the past, the moribund planned economy has failed to commercialize the country's scientific and technical achievements efficiently, let alone to market them overseas.

The group, rallied around CNTIC, will comprise trading, financing, research, design and manufacturing firms.

Tong said detailed negotiations with the State Science and Technology Commission on the establishment of the group are under way.

"It's only natural to set up such a group when China's growing technology exports have intensified demand for a sustained supply of high value-added products," he said.

It will be the first of such groups in China to cover a wide range of industries.

It even pools aerospace and military units seeking to market their hi-tech non-military products.

The impending birth of the group points up CNTIC's strategic shift to selling more high value-added machinery and electronics products, as well as equipment systems.

The government has also decided to allocate a certain amount of discount loans and export credits to support exports in this regard.

Tong said CNTIC will launch another subsidiary later this month to boost the export of equipment systems.

The CNTIC International Trade Company, which may turn out to be a shareholding one, will co-operate closely with domestic design, manufacturing and construction units in the sector.

Tong predicted CNTIC's actual exports will top \$100 million this year, versus \$76 million in 1992.

In fact, the company's contractual export volume in the first 4 months this year surpassed \$100 million.

Tong said he was upbeat about a double-digit growth rate for his company's exports this year.

"We will endeavour to acquire more support from Chinese and foreign banks, while positively investing in the banking fraternity this year," Tong said.

He did not explain how.

In another strategic move, his company will tap natural resources and hi-tech exports in China's southwest and northwest regions.

The regions, although trailing behind coastal areas in foreign trade, have clustered the bulk of China's hi-tech military plants and natural resources.

CNTIC has signed agreements with Inner Mongolia for across-the-board co-operation.

Tong disclosed that CNTIC and the Baotou Steel Complex, one of China's largest steel producers, will set up a joint venture trading company in Germany this year.

Tong will also visit Xinjiang Uygur Autonomous Region, Shaanxi Province and Guangxi Zhuang Autonomous Region soon to cement bilateral co-operation that will promote border trade with Central and Southeast Asia.

CNTIC will open representative offices in Hohhot, Urumqi and Beihai this year.

So far, most of the company's subsidiaries and offices have been set up in coastal areas.

CNTIC's exports end up mainly in Southeast Asia and South Asia.

Tong said North Africa and the Commonwealth of Independent States will be another two key markets to be exploited this year.

China's technical exports mainly fall into the energy, building materials, chemical and petrochemical sectors.

Tong said his company is also ready to co-operate with big-name international engineering companies to jointly bid for projects in a third nation.

Turning to imports, he predicted the prospects are better than last year.

In the first 4 months, CNTIC's import contracts were valued at \$1.58 billion, against \$3.5 billion for all of 1992.

"Our technical imports will further grow over last year as the national economy continues to expand."

He said his company would increase imports for large projects in the raw materials, communications, energy and telecommunications sectors this year.

CNTIC has imported \$45 billion worth of overseas technologies and equipment since its establishment 40 years ago.

Government Officials Speak at World Telecommunications Day Symposium

*40100082A Beijing CHINA DAILY in English
18 May 93 p 1*

[Article by staff reporter Xie Liangjun: "China on Line for Telecomm Success"]

[Text] China had plenty to celebrate during the 25th World Telecommunications Day yesterday.

Zhu Gaofeng, Vice-Minister of Posts and Telecommunications, said in the first four months of this year the telephone sector recorded a massive growth rate of 71.6 percent over the same period last year.

Last year it enjoyed a 49.5 percent rise, compared with 40.4 percent in 1991.

Zhu said by the end of April the country's total telephone exchange capacity—including public, private and rural phone networks—had exceeded 30 million lines.

Ranking among the world's top ten largest phone systems, he said some 67.4 per cent of the lines are digital.

Zhu, who was speaking at a symposium sponsored by the Ministry of Posts and Telecommunications in Beijing, renewed pledges to continue the high speed of growth in the sector.

Government officials predict the country's telecomm industry will grow much faster than other sectors in the national economy.

Zhu said at the symposium that China is now enjoying a sustained, stable and high-speed development period in telecommunications.

However, China's telecommunications still can not satisfy the increasing demand, prompting government officials to call for even faster expansion.

A high-ranking official of the State Council's Economic and Trade Office said that telecommunications, along with transportation, has become one of China's major pillars in its drive for a sustained and stable economic development.

He said there is room for further improvement in telecommunication services and its technological standards.

He stressed that the government will continue to adopt a series of preferential policies to back up the telecommunications sector.

China plans to increase its total telephone exchange capacity to above 100 million lines by 2000.

It expects that by then every 100 Chinese will have 5 to 6 telephones.

In provincial capitals, coastal open cities and economically developed regions, the phone coverage will reach 30 to 40 percent, with most urban households having a phone.

At present, Beijing, Haikou, Hangzhou and Guangzhou have the country's highest phone coverage rates, with 15 to 20 phones per 100 people.

China is expected to become one of the world's largest telecomm markets by the turn of next century. It is drawing more overseas telecomm giants to the country to explore business opportunities and to set up joint ventures to manufacture telecomm equipment.

Scientific Knowledge Profitable, Says Jiang Zemin
40100081A Beijing CHINA DAILY in English
15 May 93 p 1

[Article by staff reporter He Jun]

[Text] Chinese President Jiang Zemin urges Party and government officials to learn more about modern science and technology, as well as economic theories, to better serve the country's modernization and market reform.

Jiang made the remark yesterday in Beijing when meeting delegates to a national conference on science and technology.

He urged the whole of Chinese society to respect knowledge and talents.

China's modernization drive needed a large number of professionals and intellectuals, he told the conference, which ended yesterday.

Scientific development should be closely linked with economic development, as well as guiding the market, Jiang said.

Chinese Premier Li Peng, who could not attend the three-day conference because of illness, sent a message calling on all scientific and technological workers in the country to earnestly follow Deng Xiaoping's assertion that science and technology represented the "top productive force."

Song Jian, Minister of the State Science and Technology Commission, told the conference that a favourable economic climate should be developed to facilitate scientific development.

He added that the existing scientific and technological system must be restructured to suit the market economy.

Song hoped this fundamental change would be achieved by the turn of the century.

More scientists and technicians should focus on improving agriculture to gain high yields, high quality and high efficiency, the basic conditions for China's existence and development.

Song said the research and promotion of modern technology in rural areas should also serve the development of township enterprises, which were playing an increasingly greater role in China's economy.

The total output of these enterprises had surpassed that of traditional agriculture last year, reaching 1,600 billion yuan (\$275 billion) and accounting for one third of China's gross national product.

He pledged to increase investment and adopt more preferential policies to further improve the living standards of China's 900 million rural population.

As China sought to re-enter the General Agreement on Tariffs and Trade (GATT), Song urged scientists to strengthen their high-tech research to improve the competitiveness of Chinese enterprises on the international market.

"The development of high-tech industry in China can only be achieved by ourselves, not by relying on foreign-funded enterprises," Song said.

He hoped high-tech products would account for 10-20 percent of China's total export volume in 2000, instead of the current 5 percent.

The minister pledged to increase funding for basic research to more than 10 percent of the country's total investment in scientific research and development.

Song also emphasized the importance of strengthening technological training, especially at the grass-roots level.

Development of China's Launch Vehicle Systems

93FE0540A Beijing HANGTIAN [SPACE FLIGHT]
in Chinese No 2, 26 Mar 93 pp 10-12

[Article by Liu Yansheng [0491 3601 3932]: "Formation, Development of China's Launch Vehicle Series"]

[Excerpts] [Editor's Note] In previous issues of this journal, a number of articles discussed some of China's launch vehicles such as the "LM-3," the "LM-4," and the "LM-2E." In order to give the reader a more complete picture of China's family of launch vehicles, we plan to publish a series of related articles in this and future issues: "Development of China's Launch Vehicle Series," the "LM-1D," the "LM-2D," the "LM-3A," the "LM-3B," the "LM-4A," and the "LM-4B." [passage omitted]

After the successful development of the "LM-3" launch vehicle, China proceeded to develop the "LM-4" and the "LM-4A." The main difference between the "LM-4" launch vehicles and the "LM-3" is that instead of using hydrogen-oxygen propellant in the third-stage engine, normal-temperature propellant is used in the third-stage as well as in the first and second-stage engines. The normal-temperature propellant has lower energy content than low-temperature propellant. To achieve enhanced payload capability, the design of the "LM-4" has incorporated certain technical measures which include increasing the thrust of the first-stage engine and lengthening the first-stage fuel tank to accommodate a larger volume of propellant. On 7 September 1988, China's first sun-synchronous experimental satellite was successfully launched by the "LM-4," which became China's second launch vehicle with high-altitude satellite launch capability.

After the U.S. "Challenger" disaster in January 1986, the major launch vehicles of the United States and the Ariane rocket of the European Space Agency suffered a series of failures, creating a situation where many commercial satellites were queuing up for the next available

launch vehicle. This presented an opportunity for China to introduce its mature rocket technology into the international satellite launch market. To seize this opportunity, Chinese rocket designers decided to develop a strap-on rocket that can carry large-tonnage satellite payloads. This design was based on the highly successful "LM-2" launch vehicle with four liquid-propellant booster rockets strapped on an elongated first stage. The new launch vehicle, which was named the "LM-2E," generated a great deal of interest both in this country and abroad. In November 1988, China and the United States signed a contract to use the "LM-2E" for launching two satellites built by the Hughes Corp. and operated by Australia. The contract specified that test flight of the "LM-2E" be completed by April 1990 prior to launching the first "AUSSAT." To develop a large launch vehicle within 18 months and to succeed on its first flight test was unprecedented in aerospace history.

The development of the "LM-2E" required finding solutions to more than 20 key technical problems such as stability of the strap-on rocket, design of the strap connections, and separation of the booster rockets. These difficult problems were solved one-by-one by a team of highly dedicated aerospace engineers and scientists. On 16 July 1990, the first flight test of the "LM-2E" was successfully conducted from the Xichang Launch Center. Subsequently, in August 1992 and December 1992, the "LM-2E" accurately carried two "AUSSATs," which were the heaviest satellites ever built, into their pre-designated orbits.

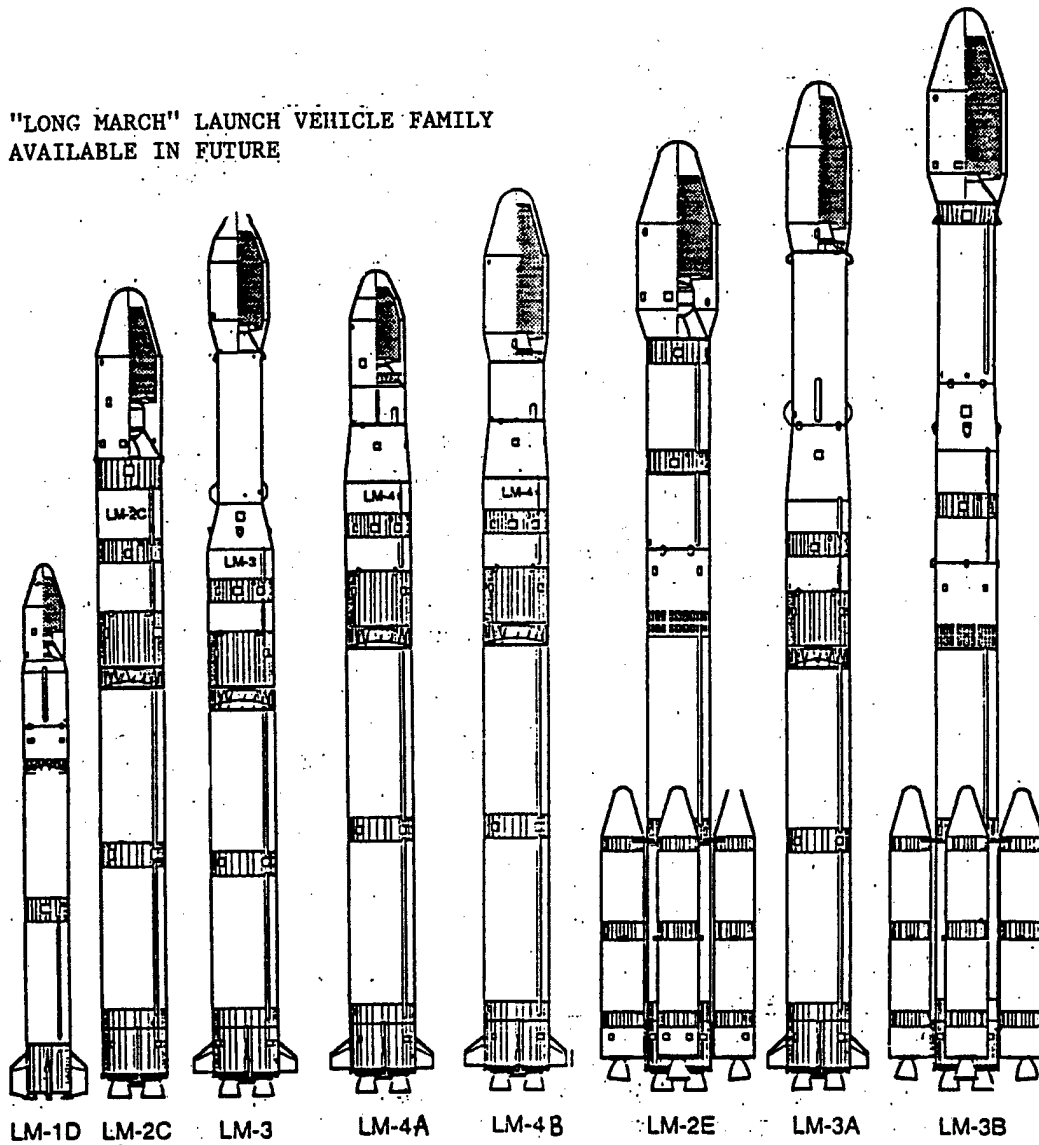
The successful development of the "LM-2E" strap-on rocket has demonstrated that an effective way to satisfy the requirements of launching different satellite payloads into different orbits is to create a new rocket by modifying existing rocket designs. In applying this principle, China is currently planning to develop the following rockets: the "LM-1D," the "LM-3A," the "LM-3B," and the "LM-4B." Completion of these rockets will give China a complete family of launch vehicles that can satisfy the satellite launch requirements for both domestic and foreign users.

Launch Records of the "LM" Family of Rockets

Sequence number	Model number	Launch date	Orbit	Result
1	LM-1	1970.4.24	LEO	Successful
2	LM-1	1971.3.3	LEO	Successful
3	LM-1A	1974.11.5	LEO	Failed
4	LM-2C	1975.11.26	LEO	Successful
5	LM-2C	1976.12.7	LEO	Successful
6	LM-2C	1978.1.26	LEO	Successful
7	LM-2C	1982.9.9	LEO	Successful
8	LM-2C	1983.8.19	LEO	Successful
9	LM-3	1984.1.29	GTO	Partially successful
10	LM-3	1984.4.8	GTO	Successful
11	LM-2C	1984.9.12	LEO	Successful
12	LM-2C	1985.10.21	LEO	Successful
13	LM-3	1986.2.1	GTO	Successful
14	LM-2C	1986.10.6	LEO	Successful
15	LM-2C	1987.8.5	LEO	Successful
16	LM-2C	1987.9.9	LEO	Successful
17	LM-3	1988.3.7	GTO	Successful
18	LM-2C	1988.8.5	LEO	Successful
19	LM-4	1988.9.7	SSO	Successful
20	LM-3	1988.12.22	GTO	Successful
21	LM-3	1990.2.4	GTO	Successful
22	LM-3	1990.3.7	GTO	Successful
23	LM-2E	1990.7.16	LEO	Successful
24	LM-4	1990.9.3	SSO	Successful
25	LM-2C	1990.10.5	LEO	Successful
26	LM-3	1991.12.28	GTO	Failed
27	LM-2D	1992.8.9	LEO	Successful
28	LM-2E	1992.8.14	LEO	Successful
29	LM-2C	1992.10.6	LEO	Successful
30	LM-2E	1992.12.21	Leo	Successful

LEO: low-earth orbit; GTO: geosynchronous transfer orbit; SSO: sun-synchronous orbit

"LONG MARCH" LAUNCH VEHICLE FAMILY
AVAILABLE IN FUTURE



Rocket	CZ-1D	CZ-2C	CZ-3	CZ-4A	CZ-2E	CZ-3A	CZ-3B	CZ-4B
Length	28	35	43.85	42	51	52.3	54.8	45.6
Lift-off wgt (T)	80	191	202	241	464	240	426	248
Lift-off thrust (T)	112	284	284	300	6000	300	600	303
LEO payload (kg)	750	2800			9000		12000	
GTO payload (kg)			1450	1500*		2300	4800	2200*
First flight	1995	1975	1984	1988	1990	1993	1995	1995

LEO: low-earth orbit

*: sun-synchronous orbit (SSO)

GTO: geosynchronous transfer orbit

An Approach to Radar Target Recognition Using Wideband Millimeter-Wave Technology

93FE0533A Shanghai HONGWAI YU HAOMIBO XUEBAO [JOURNAL OF INFRARED AND MILLIMETER WAVES] in Chinese Vol 11 No 6, Dec 92 pp 435-440

[Article by He Songhua [0149 2646 5478] and Guo Guirong [6753 2710 5554] of the Department of Electronic Technology, Changsha Institute of Technology (University of Science & Technology for National Defense), Changsha, Hunan 410073: "Approach to Radar Target Recognition by Wideband Millimeter-Wave Technology"; MS received 13 Jul 91, revised 29 Dec 92]

[Text] Abstract

A method of feature extraction and target recognition using wideband millimeter-wave technology is presented. It is shown that when illuminated by millimeter waves, a radar target can be modeled as an extended object consisting of multiple scattering centers. As long as the transmitted signal has sufficient bandwidth, the method can be used to extract such information as the spatial distribution of the scattering centers and the target features from the received signal. Simulation results show that this method is effective for recognizing complex targets in the high-frequency region.

Introduction

Radar target recognition is an important area of high-technology research and development. Past research work has been primarily focused on targets in the low-frequency region; very few articles on target recognition in the high-frequency (HF) band are found in the literature. With recent advances in the research of millimeter-wave propagation and the development of millimeter-wave high-power equipment, the application of millimeter-wave technology has been extended to such areas as precision terminal guidance; such applications impose the requirement of automatic target recognition in an environment with strong ground clutter. Since the wavelength of millimeter waves corresponds to the HF band, the scattering field of a target illuminated by millimeter waves can be modeled by synthesizing the fields of many scattering centers which reflect the physical characteristics of the edges and corners of the target. In this paper, the multiple-scattering-center model is used to study the frequency response of the target and methods for extracting the range profile using the FM continuous-wave response, processing the polarization of the range profile, and pattern recognition based on the range profile. These methods have both theoretical and practical significance in solving the problem of target recognition for millimeter-wave radar and weapons systems.

1. Extraction of Target Information From the Frequency Response of the Scattering Centers

The distribution of the scattering centers and the target features can be extracted from the amplitude and phase

information of the received signal of an HF multi-band radar. Assume that the incident wave is a linearly polarized plane wave whose incident field is:

$$E_i = E_0 \cdot e^{-jkz}, \quad (1)$$

For simplicity, the time factor $e^{j\omega t}$ in equation (1) and in subsequent equations is omitted; the wave number is $k = 2\pi/\lambda$, where λ is the wavelength. The backscatter field of the signal after being received by a linearly polarized antenna is:¹

$$E(k, z) = \left(\frac{e^{jkz}}{z} \right) \cdot \sum_{n=1}^N A_n(k) \cdot e^{j2kD_n}, \quad (2)$$

where N is the number of scattering centers, and D_n is the range difference between the n th scattering center and the reference point z . When k varies within a small range, the HF response of the target can be approximated by:²

$$A_n(k) = A_n \cdot e^{r_n k} \cdot e^{j\theta_n}, \quad (3)$$

where r_n, θ_n are features which correspond to the types of scattering centers (e.g., sharp point scattering, edge diffraction, etc.). For a fixed value of z , the factors related to z can be neglected:

$$E(k) = \sum_{n=1}^N A_n \cdot e^{j\theta_n} \cdot e^{(r_n + jd_n)k}, \quad (4)$$

where $d_n = 2D_n$, and $\xi_n = r_n + jd_n$ is called the spatial frequency. By sampling the values of k in equation (4), i.e., by letting $k_i = k_0 + i\Delta k$, one obtains:

$$E_i = \sum_{n=1}^N A_n \cdot e^{j\theta_n} \cdot e^{\xi_n k_n} e^{\xi_n i\Delta k}, \quad (5)$$

Equation (5) can be solved using the Prony method³ to yield the values of D_n, r_n and θ_n , but the disadvantage of the Prony method is that it degrades in the presence of noise. A more practical method would be to apply FFT [fast Fourier transform] to the sequence E_0, E_1, \dots, E_M , and then determine the spatial distribution D_n by locating the peak of the FFT spectrum. Therefore, equation (5) can be rewritten as:

$$E_i = \sum_{n=1}^N A_n \cdot e^{j(\theta_n + d_n k_0)} e^{r_n(k_0 + i\Delta k)} e^{jd_n \Delta k i}; \quad (6)$$

When k varies within a narrow range,

$$e^{r_n(k_0 + i\Delta k)}$$

can be regarded as a constant, hence equation (6) can be interpreted as the sum of N complex sine waves whose frequencies are $d_n \Delta k$. According to the Nyquist sampling theorem, the sampling interval Δk in the frequency domain must satisfy the condition:

$$\Delta k \leq \frac{1}{2} \cdot \frac{2\pi}{|D_n|_{\max}} \leq \frac{\pi}{L}, \quad (7)$$

where L is the dimension of the target. The frequency resolution of the FFT (i.e., the distance between the spectral lines) is:

$$\Delta = C / (2M \cdot \Delta f) = C / (2\Delta F) \quad (8)$$

where Δf is the frequency difference corresponding to Δk , C is the speed of light, and ΔF is the total bandwidth of the multi-band signal.

The FFT spectrum represents the distribution of the scattering centers projected onto the radar range axis; it is called the range profile of the target.

2. Extraction of Information of the Scattering Centers From the FM Continuous-Wave Response

A commonly used waveform that can provide information on the range distribution of the multiple scattering centers is the wideband linear FM continuous waveform. Let the modulation period be T_p , the scan bandwidth be ΔF , t_m be the time variable relative to the starting time of m th scan, then the transmitted signal with this modulation period is given by:

$$e_i(m, t_m) = A \cdot \cos \left[2\pi \left(f_0 + \frac{\Delta f}{2T_p} \cdot t_m \right) \cdot t_m + \varphi_m \right], \quad (9)$$

Assume that the local oscillator of the first-stage mixer of the receiver is coherent with the transmitted signal and has a linear FM continuous waveform with the same parameters; also, assume that the radar range of the n th scattering center is R_n , then the demodulated target signal is

$$x(m, t_m) = \sum_{n=1}^N A_n \cdot \cos(2\pi \cdot f_n \cdot t + \theta_{mn}), \quad (10)$$

$$f_n = (\Delta F / T_p) \cdot (2R_n / C) - f_{01}, \quad (11)$$

In equation (11), f_{01} is the frequency shift produced by multi-stage mixing (i.e., converting the signal into a baseband signal). By sampling the signal indicated in equation (10) and applying FFT analysis, it is possible to estimate the values of R_n based on the location of the peak of the spectrum. Let the sampling frequency be f_s

and the number of samples be $M = f_s \cdot T_p$, then the range resolution that can be achieved by the FFT is:

$$\Delta = \left(\frac{f_s}{M} \right) \cdot \left(\frac{T_p}{\Delta F} \cdot \frac{C}{2} \right) = \frac{C}{2\Delta F}, \quad (12)$$

Comparison of equation (12) with equation (8) shows that they are in complete agreement. The advantage of the millimeter band is that a wider bandwidth ΔF can be used to provide higher spatial resolution between the scattering centers and thus determine the fine structure of the target.

3. Method of Polarization Processing of the Range Profile

High resolution implies that a target generally occupies many range cells; therefore, one cannot use the concept of a point target to describe its polarization characteristics. From the one-dimensional range profile one can isolate the strong scattering centers of the target in different range cells; each strong scattering center can produce a polarization scattering matrix which can be transformed, analyzed and matched to known patterns to obtain a basic feature matrix that indicates the type of the scattering center. By synthesizing the information from many scattering centers, it is possible to obtain the features of the overall target structure. The scattering matrix S of commonly encountered scattering bodies satisfies the condition of reciprocal symmetry, i.e.,

$$S = R(\psi) \cdot T(\tau_m) \cdot S_d \cdot T(\tau_m) \cdot R(-\psi), \quad (13)$$

$$S_d = \begin{bmatrix} a_1 & 0 \\ 0 & a_2 \end{bmatrix}, \quad (14)$$

$$T(\tau_m) = \begin{bmatrix} \cos \tau_m & -j \sin \tau_m \\ -j \sin \tau_m & \cos \tau_m \end{bmatrix}, \quad (15)$$

$$R(\psi) = \begin{bmatrix} \cos \psi & -\sin \psi \\ \sin \psi & \cos \psi \end{bmatrix}; \quad (16)$$

For reflections from a three-sided body, $a_1 = a_2 = 1$; for reflections from a double plane, $a_1 = 1, a_2 = -1$; for edge diffraction, $a_1 = D_s, a_2 = D_h$; for scattering from the tip of a cone, $a_1 = jD_1, a_2 = D_2$; etc. Due to the effects of propagation, measurement errors and clutter noise, the reciprocal symmetry condition of the S matrix generally no longer holds. If the actual measured polarization matrix of a scattering center is

$$\hat{S} = \begin{bmatrix} C_1 & C_2 \\ C_3 & C_4 \end{bmatrix}, \quad (17)$$

an artificial correction is applied to S [caret over S] to ensure that condition of reciprocal symmetry is satisfied:

$$\hat{S}' = \begin{bmatrix} C_1 & \frac{1}{2}(C_2 + C_3) \\ \frac{1}{2}(C_2 + C_3) & C_4 \end{bmatrix}, \quad (18)$$

However, one cannot decompose S' [caret over S] as in equation (13). For the case of basic scattering centers such as multiple reflections, edge diffraction and scattering from sharp corners, $\tau_m = 0$; hence the unknowns a_1 , a_2 and ψ can be chosen so that the matching error between S and S' [caret over S] is minimized. The attitude of the scattering body can be determined from the value of ψ [caret over ψ], and the values of (a_1 [caret over a], a_2 [caret over a]) are used to match the feature vectors (a_1 , a_2) of the basic scattering bodies, i.e.,

$$\cos\theta = \left| \frac{a_1 \hat{a}_1 + a_2 \hat{a}_2}{\sqrt{(a_1^2 + a_2^2)(\hat{a}_1^2 + \hat{a}_2^2)}} \right|, \quad \left(0 \leq \theta \leq \frac{\pi}{2} \right) \quad (19)$$

In equation (19), a small value of θ indicates good match between the unknown body and the basic scattering body. Computer simulation results show that for the case of four basic scattering bodies, i.e., the three-sided body, the double plane, the edge and the sharp corner ($D_s = 0.5$, $D_h = 1.5$, $D_1 = 0.286$, $D_2 = -1$) distributed at the four corners of a $3 \times 3 \text{ m}^2$ square, correct results were obtained at a range resolution of $\Delta = 0.3 \text{ m}$ by matching the polarization matrix obtained from the range profile with the scattering matrix of the known scattering bodies under four different polarization combinations (HH, HV, VH, VV).

4. Pattern Recognition Based on the Target Range Profile

The amplitude spectrum produced by the FFT reflects the distribution of the scattering centers projected onto the radar range axis; it is called the one-dimensional range profile of the target. The range profile contains a considerable amount of target information, even in a single-polarization channel (e.g., HH). Figure 1 shows the range profiles of two simulated ground targets (a tank and a truck) with the radar located in front of the target at 0° azimuth and 10° elevation. The profiles clearly exhibit the fine structures of the tank and the truck, and these structural features can be used for target recognition.

When the attitude angle of the target changes, the projected locations of the scattering centers on the range axis also change; therefore, it is difficult to recognize the range profile without knowing the attitude angle. In the simulation process of this paper, we have solved the following problems to facilitate range-profile recognition:

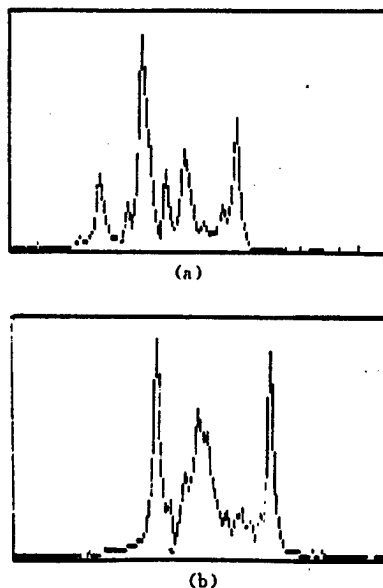


Figure 1. One-Dimensional Range Profiles of Targets (FFT Amplitude Spectrum) (a) tank (b) truck ($\Delta F = 500 \text{ MHz}$)

(1) Constructing target models. This involves generating a distribution map of the 3-D scattering centers of the four basic targets projected onto the range axis at different attitude angles.

(2) Constructing target feature models. This involves extracting a series of features from the range profiles of known targets; these features include the radial length, the number of spectral peaks, and the sum of squares of the range differences between the peak locations and the range centroid. In addition, a data base of classification rules has also been established using the method of sequential deduction;⁴ these rules reflect the constraint relationships between the different features.

(3) Pattern classification. This involves sequentially comparing the feature values of the range profiles of the unknown target against the threshold of each classification rule of the data base.

Simulation results show that for the four targets being considered, if a model is constructed for a constant elevation angle of 10° and azimuth angles varying from 0° to 360° at 30° intervals, then the probability of correct classification of a range profile with unknown azimuth angle (i.e., arbitrarily sampled azimuth) is higher than 85 percent.

5. Unique Features of Wideband Millimeter-Wave Target Recognition Technique

(1) Like light waves, millimeter waves propagate nearly along a straight line. Therefore, in general the range profile of a target reflects only the structural characteristics of the illuminated surface and it changes with the

attitude angle; it provides information on the fine structure of the target but does not contain information of the coarse structural characteristics at low radar frequencies.

(2) The target recognition technique is based on the theory that the target can be represented by multiple scattering centers distributed in a particular pattern; the scattering centers play a similar role in HF target recognition as the poles do for low-frequency radar targets. The success of this technique depends on the results of analysis and research on the distribution of the scattering centers, the frequency response and the polarization characteristics.

(3) The high range resolution provided by the wideband system provides the capability of isolating the strong scattering centers of the target; the higher the resolution, the lower the power of clutter and noise from elements around the scattering centers. Therefore, the HF target recognition technique has good clutter-rejection and noise-rejection capability.

(4) Since the variation of the feature values with attitude angle is non-random, traditional statistical pattern recognition techniques are not effective in classifying complex targets. To classify such targets, it is necessary to construct dynamic models of the feature values which are more complex than the statistical models (mean feature value, covariance matrix, etc.).

(5) The conventional method of FFT spectral estimation can achieve the inherent resolution of wideband waveforms; it is also simple and easy to implement.

6. Conclusion

Studies of pattern recognition techniques using the range profile and the polarization processing method show that application of millimeter-wave technology in target recognition is quite feasible and provides high range resolution. As an extension of this work, the potential of using wideband waveforms to provide good doppler resolution and angular resolution should be exploited to further enhance the application of this technique in radar target recognition.

References

1. Songsung, H., IEEE TRANS. ANTENNAS PROPAG., 1968, 16 (1): 99.
2. Hurst, M. P., AD-P001105, 245-257.
3. Brittingham, E. K., PROC. IEEE, 1985, 68 (1): 13-19.
4. He Songhua, Guo Guirong, MOSHI SHIBIE YU REN-GONG ZHINENG [PATTERN RECOGNITION AND ARTIFICIAL INTELLIGENCE], 1992 (2): 135-140.

Isolation and Characterization of a Human cDNA of Pro-Urokinase

40091010A Beijing BEIJING DAXUE XUEBAO [ACTA SCIENTIARUM NATURALIUM UNIVERSITATIS PEKINENSIS] in Chinese Vol 29 No 2, Mar 93 pp 209-213

[English abstract of article by Hu Meihao [5170 5019 3185] of the Department of Biology, Peking University]

[Text] The cDNA encoding human pro-urokinase has been isolated from a cDNA library prepared from human placenta cells. Two pairs of probes have been used for hybridization. These probes are made by in vitro extension of synthesized oligonucleotides. Characterized by restriction endonuclease map southern blot, and sequencing, this cDNA covers the complete coding sequences of the matured urokinase of 411 amino acids and of 20 amino acids of the signal peptide. It also covers the 3' untranslated region and the 5' untranslated region of 95 nucleotides.

Channel-Forming Activity at Planar Lipid Bilayer of the Membrane Active Polypeptide B Form Venom of *Bungarus Fasciatus*

40091010B Shanghai SHENGLI XUEBAO [ACTA PHYSIOLOGICA SINICA] in Chinese Vol 44 No 6, Dec 92 pp 533-540

[English abstract of article by Shi Yuliang [2457 3768 2856], Wang Wenping [3769 2429 5493], et al. of the Shanghai Institute of Physiology, Academia Sinica, Shanghai 200031]

[Text] Using planar lipid bilayer formed by lecithin and cholesterol (20 and 5 mg/ml respectively in N-decane) the channel-forming activity of the membrane active polypeptide B (BMAP B) from the venom of *Bungarus fasciatus* was investigated. Under the existence of a voltage or a salt concentration gradient between two sides of the bilayer, unit conductance fluctuation and a decrease in steady state resistance accompanying BMAP B incorporation and channel formation were observed. By measuring the reversal potential in an asymmetric solution, the selectivity of the BMAP B-channel was estimated to have a value of $P_K/P_{Cl} = 1.4$. Divalent cations, such as Ba^{2+} , Ca^{2+} inhibited the channel activity as they did in biomembranes. These data might provide an explanation for the depolarizing effect of the membrane active polypeptide on the native membranes.

Key words: *bungarus fasciatus* venom membrane-active polypeptide (BMAP); planar lipid bilayer; ion channel; unit conductance fluctuation; divalent cations

Design and CD Study of α/β Alterable Peptides

40091010C Shanghai SHENGWUHUAXUE YU SHENGWUWULI XUEBAO [ACTA BIOCHIMICA ET BIOPHYSICA SINICA] in Chinese Vol 24 No 4, Jul 92 pp 317-326

[English abstract of article by Xu Mei [1776 2734], Zhang Ying [1728 7751], and Lu Zixian [7627 1311 6343] of the Shanghai Institute of Biochemistry, Academia Sinica, 200031]

[Text] An α/β alterable peptide has been designed, synthesized and purified. This peptide has both high α -helix conformational potential and β -pleated sheet conformational potential. According to the principles of peptide design, different methods were used to analyze interactions that stabilize the structure of this model peptide and its chain. Different solutions have been used to mimic the microenvironment of the peptide in its natural state as a protein. The CD study on the conformations of three peptides refracted that α/β alterable peptide will format α -helix or β -pleated sheet according mainly to the solution surrounding it and the residues immediately join to it. The results were compared with the design.

Key words: α/β Alterable peptide; Peptide design; CD (circular dichroism)

Synthesis of Insulin Analogues With Deletions at the Helical Region of the A Chain

40091010D Shanghai SHENGWUHUAXUE YU SHENGWUWULI XUEBAO [ACTA BIOCHIMICA ET BIOPHYSICA SINICA] in Chinese Vol 24 No 6, Nov 92 pp 503-508

[English abstract of article by Yang Shizhen [2799 1102 3791], Huang Yiding [7806 0001 0002], et al. of the Shanghai Institute of Biochemistry, Academia Sinica, 200031]

[Text] Using p-alkoxy benzylate hydroxyl resin as the resin support and Fmoc- for the protection of α -amino groups, A21 modified A chain of porcine insulin and its two helical region deleted derivatives were prepared, and subjected to recombination with the natural B chain to give corresponding insulin analogues. The observations that those analogues showed definite and appreciable activities in both *in vivo* and receptor binding suggested that A21 can be replaced by simple amino acid residues and that not only can the A chain with damaged structural integrity gradually combine with the B chain but that the combination products can also show definite biological activity.

Molecular Cloning and High Expression of Yeast PHO 85 Gene in *E. coli*

40091010E Shanghai SHENGWUHUAXUE YU SHENGWUWULI XUEBAO [ACTA BIOCHIMICA ET BIOPHYSICA SINICA] in Chinese Vol 24 No 6, Nov 92 pp 523-530

[English abstract of article by Zhong Hualin [6988 5478 3829], Li Boliang [2621 0130 5328], and Ao Shizhou [2407 0013 3166] of the National Laboratory of Molecular Biology, Shanghai Institute of Biochemistry, Academia Sinica, 200031]

[Text] PHO 85 is a negative regulator of the repressible acid phosphatase gene system of *Saccharomyces cerevisiae*. A 0.9 kb-DNA fragment containing the PHO 85 coding region has been amplified by PCR from yeast chromosomal DNA and cloned in the plasmid vector pUC18 and analyzed by restriction mapping, Southern hybridization and DNA sequencing.

The expression plasmid of PHO 85 gene under the control of λ PL promoter was constructed and transformed to *E. coli* harboring temperature sensitive repressor gene. The PHO 85 protein product was obtained from the cells induced at 42°C and a new protein of approximately 35 kd was present in SDS-PAGE. The induced PHO 85 protein existed as inclusion body represents about 35 percent of the total cellular proteins. Through isolation and purification of inclusion bodies more than 72 percent purity of PHO 85 protein was obtained. The partially purified PHO 85 protein was subjected to sequential NH₂-terminal analysis. The first 16 amino acids of the PHO 85 product are the same as that derived from the nucleotide sequence. The cloned PHO 85 protein can be used to study the regulatory mechanism of acid phosphatase genes.

The ¹H Resonance Assignment of Modifier of 16-Peptide Fragment in Rat TGF- α Using 2D NMR

40091010F Shanghai SHENGWUHUAXUE YU SHENGWUWULI XUEBAO [ACTA BIOCHIMICA ET BIOPHYSICA SINICA] in Chinese Vol 24 No 6, Nov 92 pp 531-538

[English abstract of article by Huang Yongren [7806 3057 0088] and Sheng Wanyun [4141 1354 0061] of the NMR Laboratory and Analysis Center of East China Normal University, Shanghai, 200062, and Xie Huiqin [6200 1979 3830] of the Shanghai Institute of Organic Chemistry, Academia Sinica, 200032; project supported by the National Natural Science Foundation of China, and State Spectrum and Atom-Molecule Physics Laboratory]

[Text] Transforming growth factors form an important basis illustrating the self-secretion phenomenon in cancer cells. The modifier 16-peptide fragment is the part of the C-terminal of rat transforming growth factor with stronger activity. In this paper, a complete proton chemical shift assignment for this fragment is carried out by means of 2D NMR techniques, such as COSY, TOCSY, DQF-COSY AND NOESY, which provides an essential foundation for elucidation of its conformation.

Synthesis of a Modified T₅P₂₅ Promoter and Its Use for High-Level Expression of IFN- α A Gene

40091010G Shanghai SHENGWUHUAXUE YU SHENGWUWULI XUEBAO [ACTA BIOCHIMICA ET BIOPHYSICA SINICA] in Chinese Vol 24 No 6, Nov 92 pp 539-544

[English abstract of article by Wang Chengyao [3076 2052 1031], Tang Jinyan [3282 6930 3508], et al. of the Shanghai Institute of Biochemistry, Academia Sinica, 200031, and Wang Qisong [3769 0796 2646] of the Institute of Genetics, Fudan University, Shanghai, 200433]

[Text] The synthesis of a modified T₅P₂₅ promoter (MT₅) was described. It was used for the expression of interferon- α A. High-level expression of this interferon in *E. coli* under the control of our MT₅ promoter up to 1.2 x 10⁹ units antiviral

activity per liter culture was obtained. It is about 4.8 times higher than that of Goeddel et al. using trp promoter.

PCR-Amplification, Cloning and Sequencing of 2F7 Monoclonal Antibody Variable Domains

40091010H Shanghai SHENGWUHUAXUE YU SHENGWUWULI XUEBAO [ACTA BIOCHIMICA ET BIOPHYSICA SINICA] in Chinese Vol 24 No 6, Nov 92 pp 581-586

[English abstract of article by Wu Wenshu [0702 2429 2579], Huang Zhenyu [7806 7201 1342], et al. of the Department of Immunology and Cell Biology, Shanghai Cancer Institute, 200032, and Li Daizong [2621 1486 1350] of the Department of Biochemistry and Molecular Biology, Shanghai Cancer Institute, 200032]

[Text] It is reported here that immunoglobulin variable domains were amplified from the genomic DNA of hybridomas against human small cell lung cancer with a set of universal 5'-oligodeoxyribonucleotides. The VHFR1 primer and JHFR4 primer used to amplify VH domains were on the FR1 site and FR4 site, respectively. The VKFR1 primer and JKFR4 primer used to amplify VK domains were on the FR1 site and FR4 site, respectively. The VK and VH domain DNA fragments amplified were cloned into pGEM-7Zf(+)/VKPCR and M13mp19 vector respectively and then sequenced, which assures us that 80 percent of clones with insert had correct immunoglobulin variable domain sequences. The primers incorporate restriction sites that allow the DNA of variable domains to be cloned for sequencing and ligation with human immunoglobulin constant domains. This technique is helpful to the cloning of immunoglobulin variable domains and construction of human/mouse chimeric antibody quickly and correctly.

Secretion of Overproduced Human Epidermal Growth Factor in *Escherichia coli*

40091010I Shanghai SHENGWUHUAXUE YU SHENGWUWULI XUEBAO [ACTA BIOCHIMICA ET BIOPHYSICA SINICA] in Chinese Vol 24 No 6, Nov 92 pp 587-589

[English abstract of article by Gan Renbao [3927 0086 1405], Huang Peiyong [7806 1014 0516], et al. of the Shanghai Institute of Biochemistry, Academia Sinica, 200031]

[Text] Using our previously constructed expression plasmid pAE-8 in *Escherichia coli* YK537, a strain capable of secretory expression of human epidermal growth factor (hEGF), we have optimized the conditions for cell culture and induction of expression.

EE-8 cells were grown in a medium containing polypepton and yeast extract and were induced for expression of hEGF under low phosphate conditions. hEGF was expressed after 2 hours of induction and secreted into the culture medium with increase of inducing time. The amount of expressed hEGF was as high as 30 mg/liter culture, when EE-8 cells

were induced in a low phosphate medium for 10 hours. About 90 percent of the total expressed hEGF was secreted into the medium.

2D-NMR Studies of α/β Alterable Peptides

40091010J Shanghai SHENGWUHUAXUE YU
SHENGWUWULI XUEBAO [ACTA BIOCHIMICA
ET BIOPHYSICA SINICA] in Chinese Vol 25 No 1,
Jan 93 pp 1-9

[English abstract of article by Xu Mei [1776 2734], Xu Lingfei [1776 0407 7378], and Lu Zixian [7627 1311 6343] of the Shanghai Institute of Biochemistry, Academia Sinica, 200031]

[Text] Two-dimensional NMR method has been used in this paper to further studies on the solution conformation of α/β alterable peptides. All the spin system of residues have been assigned and preliminary models have been established according to the NOE's among protons, that is: PEP-1 formed a weak turn in water and a weak helix in TFE, PEP-3 formed a partial sheet in DMSO. Summarizing the results of CD and 2D-NMR, a further discussion on the solution conformation of α/β alterable peptides has been given.

Key words: Alterable peptide; 2D-NMR; Protein folding

Solution Conformation Studies on Bradykinin by 2D-NMR and Molecular Dynamics

40091010K Shanghai SHENGWUHUAXUE YU
SHENGWUWULI XUEBAO [ACTA BIOCHIMICA
ET BIOPHYSICA SINICA] in Chinese Vol 25 No 1,
Jan 93 pp 11-18

[English abstract of article by Yang Weiwen [2799 0251 2429], Wang Sanshan [3769 0005 1472], et al. of the Shanghai Institute of Biochemistry, Academia Sinica, 200031; project supported by the National Natural Science Foundation of China]

[Text] The conformation of bradykinin in DMSO- d_6 solution was studied by use of various 2D-NMR techniques. The assignments of different spin systems and chemical shifts were accomplished using COSY, sensitive relayed-COSY combined with NOESY spectra. The molecular structure was generated after restrained molecular dynamics calculations. NH_3 -Arg-Pro-Pro is relatively flexible in DMSO, while the six residues at C-terminal, involving two turns, were compacted.

Key words: Two-dimensional NMR; Bradykinin; Restrained molecular dynamics

In Vitro Inhibition of Indirect Immunotoxin Mediated by Monoclonal Antibody on Human Melanoma Cell Line

40091010L Shanghai SHENGWUHUAXUE YU
SHENGWUWULI XUEBAO [ACTA BIOCHIMICA
ET BIOPHYSICA SINICA] in Chinese Vol 25 No 1,
Jan 93 pp 39-43

[English abstract of article by Zhang Zuchuan [1728 4371 0278], Zhang Ruping [1728 5423 1627], et al. of the Shanghai Institute of Biochemistry, Academia Sinica, 200031]

[Text] An indirect immunotoxin (SAMIg-TCS), which was composed of sheep anti-mouse immunoglobulins antibody (SAMIg) and trichosanthin (TCS), a single chain ribosome-inactivating protein, has been constructed. Human melanoma cells (M_{21}) were inhibited effectively by SAMIg-TCS mediated by anti-human melanoma monoclonal antibody (Ng37). The IC_{50} of SAMIg-TCS mediated by Ng37 and free TCS was 2×10^{-9} M and 5×10^{-7} M respectively. The indirect immunotoxin mediated by Ng37 was 250-fold more cytotoxic to M_{21} cells than free TCS. Whereas, SAMIg-TCS mediated by Ng37 showed an IC_{50} of 1×10^{-6} M to human HeLa cells and it was 500-fold less cytotoxic to M_{21} cells. The results showed that the indirect immunotoxin is a potent and specific, common antitumor agent when combined with a specific antitumor monoclonal antibody.

Enhancement of Thermostability of Subtilisin E by Means of Protein Engineering

40091010M Shanghai SHENGWUHUAXUE YU
SHENGWUWULI XUEBAO [ACTA BIOCHIMICA
ET BIOPHYSICA SINICA] in Chinese Vol 25 No 1,
Jan 93 pp 51-57

[English abstract of article by Wang Xianshun [3769 6343 5293], Wang Peizhi [3769 1014 0037], et al. of the Department of Biology, University of Science and Technology of China, Hefei 230026, and Bi Ruchang [3968 3067 2490] of the Institute of Biophysics, Academia Sinica, Beijing 100101. This is an "863" Plan key project.]

[Text] A synthesized mutagenic primer (5'-CTTACGGCGCCTATAGCGGATCGT-3') [GGCGCC has NarI under underlining; letters AGC are overlined with Ser above overline] of apr E (gene of subtilisin E), associated with gapped duplex M13mp18-apr E DNA, was extended and ligated with M13mp18 DNA. Then it was transformed to appropriate hosts to obtain a mutant, M13mp18-aprE'. Results of gel electrophoresis analysis of the wild type M13mp18-apr E and the mutant M13mp18-aprE' DNA, and digestion of endonucleases Sall and NarI show that the production of mutant aprE'

(218 Asn-Ser) was successful. Then, a recombinant pPZW8890 was produced by recombination of aprE' gene with a plasmid of *Bacillus subtilis*, pPZW103. After transformation of pPZW8890 to *Bacillus subtilis* DB104, the mutated subtilisin was secreted. The thermostability of subtilisin E' was four times that of the wild type, subtilisin E.

Key words: Thermostability; Subtilisin E; Gapped duplex DNA; pPZW8890

Additional Details on 1992 High-Tech Import, Export Figures

93P60241A Beijing JISUANJI SHIJIE [CHINA COMPUTERWORLD] in Chinese No 15, 21 Apr 93 p 1

[Article by Liu Jiuru [0491 0046 1172]: "Nation's High-Tech Product Exports Continue To Grow"]

[Editorial Report] Additional details not included in an earlier report on the State S&T Commission's release of China's 1992 high-tech product export and import figures [see JPRS-CST-93-009, 13 May 93 p 1] are as follows: Among exports of computers and communications products, the leading high-tech export components, computer parts and color TV receivers together accounted for US\$500 million in export volume. The 1992 high-tech product trade deficit of US\$6.716 billion (total high-tech imports of US\$10.712 billion less total high-tech exports of US\$3.996 billion) is only slightly (US\$156 million) higher than the figure for 1991. The relative high-tech product trade deficit (defined as ratio of high-tech product trade deficit to high-tech product export volume) decreased from 227.8 percent for 1991 to 168 percent for 1992.

U.S. Firm AMNET Introduces Integrated WAN Technology to China

93P60241C Beijing JISUANJI SHIJIE [CHINA COMPUTERWORLD] in Chinese No 16, 28 Apr 93 p 5

[Article by Ying Zi [5391 1311]: "AMNET Introduces Integrated Wide-Area Network Technology Suited to China"]

[Summary] The U.S. firm AMNET, a specialist in network technologies, by invitation came to China on 22-29 March to introduce to domestic users the firm's fast packet switching and frame-relay wide-area network (WAN) technologies as well as its Nucleus 7000 series of frame-transmission network products. AMNET's forte is frame-relay and X.25 WAN technologies, and AMNET indicated that its Nucleus 7000 products—in comparison to similar products from other firms—are more suited to aiding Chinese firms fulfill their stated targets. AMNET, a privately held corporation, has experience in providing U.S., European, Asian-Pacific, and South American network users and equipment firms with RISC-based WAN systems and intelligent search techniques.

Wanfang Markets China Enterprise, Corporation, and Product Database

93P60241B Beijing JISUANJI SHIJIE [CHINA COMPUTERWORLD] in Chinese No 16, 28 Apr 93 p 1

[Article by Liu Jing [0491 5464]: "Wanfang Co. Markets New Edition of Enterprise Information Database"]

[Summary] The Beijing Wanfang [8001 2455] Data Co., established only 2 months ago by the China S&T Information Research Institute, recently marketed a new (1993) edition of the China Enterprise, Company (Corporation),

and Product Database (CECDB). This new Chinese-language edition of CECDB, which answers the questions "Who Produces What?" and "Who Sells What?" on the Chinese market, includes information on 80,000 domestic enterprises, companies, and corporations—30,000 more than listed in the 1992 version, put out by the original China S&T Information Research Institute's Technical and Economic Data Division—as well as on their product lines. The new (1993) English-language version of CECDB has information on 28,000 domestic firms, 10,000 more than listed in the 1992 version. Wanfang has also marketed a CECDB optical disk, with full information on the 80,000 firms. In addition, Wanfang will shortly unveil two new products: a technical achievements database (1993 version) applicable to China and listing 80,000 transferable achievements, and a China Scientific Research Organizations Database (1993 version) with information on over 7,000 leading domestic research organizations. Earlier versions of CECDB have exerted a considerable influence in the United States, Britain, Canada, Switzerland, Taiwan, and Hong Kong.

Design, Implementation of Knowledge-Based Operating Language

93P60237A Shenyang XIAOXING WEIXING JISUANJI XITONG [MINI-MICRO SYSTEMS] in Chinese Vol 14 No 4, Apr 93 pp 26-31

[Article by Liao Minghong [1675 2494 1347], Guo Fushun [6753 4395 7311], et al. of Harbin Institute of Technology, Harbin 150006: "Design and Implementation of a Knowledge-Based Operating System," supported by research grant from State 863 Plan; MS received 13 Jul 92]

[Abstract] A knowledge-based machine is a special-purpose computer used to manage a knowledge-based production system. The knowledge-based operating language (KBL) presented here is intended to provide a means for users to organize and manage the knowledge-based machine, known as HITKBM90 [Harbin Institute of Technology Knowledge-Based Machine, 1990], that we designed and developed under an 863 Plan grant. In this paper, the design of HITKBM90 is introduced, and the design and implementation of the KBL is discussed in detail.

HITKBM90, whose basic modes consist of the combination of a rule base + database(s) + inference engine, has as its user interface the KBL and its environment; this environment includes the knowledge-based system working environment and the KBL support environment. The architecture of HITKBM90 is shown schematically in Figure 1 below, while Figure 2 (not reproduced) shows the machine's operating process (flow charts for initiation and inference). KBL text consists of the following components: a basic character set, including the 26 English-alphabet letters, 10 numerals, and 15 other symbols (such as +, -, *, :, =, <, and >); identifiers; four basic data types, including integer, real number (such as 1.5E-10), character string, and Boolean expression (true and false); three composite data types, including array, record, and pointer; the four algebraic operations; nine Boolean

operations; basic primitives, consisting of rule-based operating primitives, database operating primitives, inferential operating primitives, and other operating primitives; and user-defined primitives (MACROs).

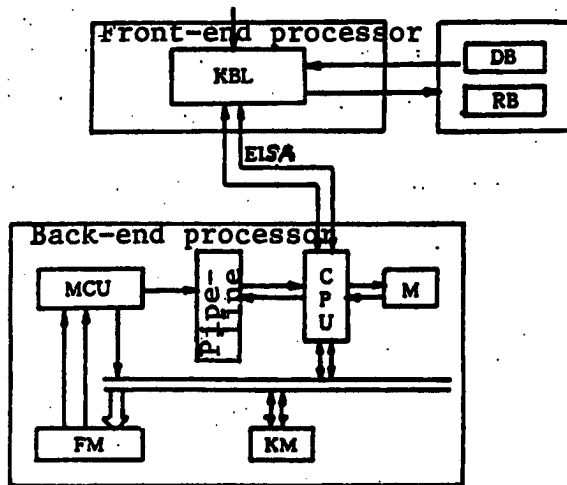


Figure 1. Architecture of HITKBM90; DB = database(s), RB = rule base, EISA = Extended Industry Standard Architecture bus, MCU = memory control unit, CPU = 32-bit central processing unit, M = local memory, FM = flag memory, KM = knowledge memory

References

1. C. L. Forgy and A. Gupta, "Preliminary Architecture of the CMU Production System Machine," in Proc. 19th Annu. Hawaii Int. Conf. System Sciences, Jan. 1986, pp 194-299.
2. A. Gupta, "Implementing Ops5 Production System on DADO," in Proc. Int. Conf. Parallel Processing, Aug. 1984, pp 83-91.
3. Jean-Luc Gaudiot, Andrew Sohn, "Data-Driven Parallel Production System," IEEE TRANSACTIONS ON SOFTWARE ENGINEERING, Vol 16, No 3, March 1990.
4. Zhang Xuehai, Liao Minghong, et al., "Research on Design of Knowledge-Based Machine HITKBM90," Zhishi Gongcheng Jinzhan [Advances in Knowledge Engineering], 1991, China Geological University Publishing House.

Nation's First Satellite GPS Applications System Operational

93P60242B Beijing RENMIN RIBAO OVERSEAS
EDITION in Chinese 5 May 93 p 1

[Article by Yuan Wen [5913 2429]: "[Nation's] First Global Satellite Positioning Applications System Became Operational Yesterday in Beijing"]

[Summary] Beijing, 4 May (ZHONGGUO XINWEN SHE)—China's first global satellite positioning applications system became formally operational today in Beijing. The Global Positioning System (GPS), also known as an automatic tracking and navigation system, was first established by the U.S. Armed Forces primarily for submarine command and battle tank applications; the technology is now being transferred for civilian use in the United States. The tracking and positioning text/graphics display system jointly developed by Beijing Jinli [6855 0448] Electronic Technology Ltd. and Beijing Yushi [1342 6018] S&T Engineering Co. has a maximum positioning accuracy of 0.5 meter. Jinli is a joint venture jointly run by the Beijing High-Technology Experimental Zone and the Taiwan Lik'enta [0448 5146 1129] Ltd. Stock Company. The first application of this domestic GPS system is the Agricultural Bank of China for its armored cars.

Utilitarian DAT Player, 5.25-Inch Erasable Rewritable Magneto-Optical Disk Unveiled

93P60242A Beijing KEJI RIBAO [SCIENCE AND TECHNOLOGY DAILY] in Chinese 26 Apr 93 p 1

[Article by Yu Zhuo [0060 0587] and Zhou Ganpu [0719 2413 2528]: "Nation's Optoelectronic Recording Technology in World's Front Ranks"]

[Summary] Beijing, 24 Apr—The Ministry of Electronics Industry held a press conference today in Beijing to introduce two new products recently developed by engineers at the [Chengdu] University of Electronic Science & Technology of China (UESTC): a "utilitarian optoelectronic digital audio tape (DAT) player/recorder" and a "utilitarian 5.25-inch erasable recordable magneto-optical disk." Both of these were certified yesterday by a panel of experts (in unanimous agreement) to meet current international standards for such products—indicating that the nation's optoelectronic recording technology is now world-class. Also at the press conference, the State Commission for Restructuring the Economy, the State S&T Commission, and the Ministry of Electronics Industry announced that China will operate a joint-stock system entity to accelerate the

industrialization, commercialization, and internationalization of these two high-tech products. Trial manufacturing at this new entity, the Shenzhen Tianji [1131 2817] Optoelectronic Technologies Industrial Ltd. Co., indicates promising results.

Experimental Research on Ultrafine (Nanoscale) Optoelectronic-Conversion Thin Film

93FE0536C Beijing KEXUE TONGBAO [CHINESE SCIENCE BULLETIN] in Chinese Vol 38 No 3, 1-15 Feb 93 pp 210-211

[Article by Wu Jinlei [0702 6930 7191], Liu Weimin [0491 1919 2404], Dong Yinwu [5516 1714 0710], Shi Ziguang [4258 5261 0342], Pang Shijin [1690 0013 3866], Zhao Xingyu [6392 5281 3768], Xue Zengquan [1331 1073 3123], and Wu Quande [0702 0356 1795] of the CAS Beijing Vacuum Physics Laboratory and the Beijing University Department of Radio and Electronics: "Experimental Research on Ultrafine Optoelectronic-Conversion Thin Film"; MS received 29 Sep 92]

[Text] [Introduction]

There are two types of basic photoemissive materials for laser pulse detection. One includes a number of alkali-metal-containing photoemissive films,¹ such as Ag-O-Cs, Cs₃Sb, [Cs]Na₂KSb, etc. Gex et al. pointed out that the semi-transparent Ag-O-Cs photocathode is the only material suitable for the study of 1.06- μ m lasers with a pulsewidth of less than 10 ps.² The other includes pure-metal thin films such as Au and Ag. Although the first type is more sensitive, it cannot operate at above 150°C, nor can it be exposed to the atmosphere. If it is exposed to air, the photoemissive film would be destroyed. These deficiencies not only pose enormous difficulties to its use, but also render it totally useless in certain situations. Although pure-metal thin films such as Au and Ag can be exposed to the atmosphere and can also operate at high temperature, their sensitivity is very low. Consequently, they also make laser pulse detection difficult.

The Ag-Ba-O film developed in this work overcomes these technical hurdles. It can be stored in air and its photoemissive property can be restored in vacuum. Moreover, this photoemissive film can operate at high temperatures and is highly sensitive. It is suitable for laser pulse detection. In this film, the ultrafine Ag particles are buried in the semiconducting BaO substrate. Ultrafine particles are particles with a diameter ranging from 1 nm to 100 nm.³ These nanoparticles have different characteristics from those discussed in atomic, molecular and solid-state physics.⁴ This Ag-Ba-O film is such a novel optoelectronic-conversion film.

1. Experimental Apparatus

The Ag-Ba-O film is prepared in a vacuum system consisting of a mechanical pump, a diffusion pump, and a sample tube, as shown in Figure 1. The system holds a vacuum of 3×10^{-5} Pa. Silver, barium and oxygen are deposited on a glass substrate using a specific technique to form an optoelectronic-conversion film where the ultrafine metal particles are buried in the semiconductor.

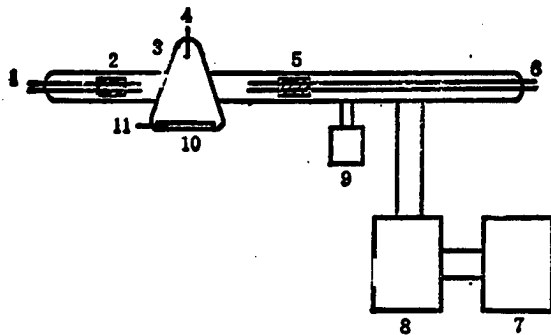


Figure 1. Film Preparation Apparatus

1, 6. Tracks; 2. Ba source; 3. Sample tube; 4. Anode; 5. Ag source; 7. Mechanical pump; 8. Diffusion pump; 9. O₂ source; 10. Thin film; 11. Cathode

To use the Ag-Ba-O film in laser pulse detection, the film must be incorporated in a dynamic laser pulse detector. During the process, the film is exposed to the atmosphere. Figure 2 shows the detection equipment, which consists of a laser, external optics, optoelectronic-conversion film, streak camera, vacuum system and test instruments. The laser is a 1.06- μm -wavelength passive mode-locked Nd:YAG laser. Each short pulse is 50 ps wide and each pulse series contains 9-11 pulses. A pulse series is emitted every 1 or 5 seconds. The energy per series is 3 mJ. The laser beam goes through an attenuator and a focusing plate before reaching the film. It may also hit the film directly. If a KTP frequency-doubling crystal is added in the external optics, the light becomes green with a wavelength of 0.53 μm . Regardless of whether it is the 1.06- μm infrared light or the 0.53- μm green light, optoelectronic emission can be detected with the streak camera.

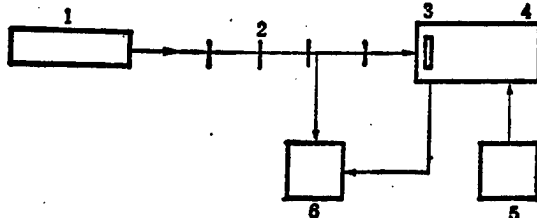


Figure 2. Laser Detection Equipment

1. Laser; 2. External optics; 3. Optoelectronic-conversion film; 4. Streak camera; 5. Vacuum system; 6. Instruments

2. Experimental Results and Conclusions

The behavior of an optoelectronic-conversion film under laser illumination is due to the multi-photon emission effect.⁵ Schelev et al. of the former USSR reported the use of a streak camera to measure the intensity distribution of a laser.⁶ They employed a 2.94- μm active mode-locked Yb-Er-Al laser to produce picosecond pulses. The mean energy per pulse is approximately 1 mJ. A PV-001 tube with an Ag-O-Cs photocathode was used to detect these pulses at 2.94 μm ; sensitivity threshold was reported to be

10⁸ W/cm². They believed that this optoelectronic emission effect could be described by a three-, four- or even five-photon process.

The medium-sensitivity Ag-Ba-O film used in this work was found to have an integrated sensitivity of 0.2 $\mu\text{A}/\text{lm}$ using a standard white light. The laser beam hit the optoelectronic film after passing through an attenuator with a transmittance of 3.3 percent. The sensitivity thresholds of the film are 6×10^7 W/cm² and 1×10^8 W/cm² for 1.06 μm and 0.53 μm pulses, respectively. These are comparable to values for the Ag-O-Cs film used by Schelev. However, the Ag-Ba-O film has been exposed to the atmosphere.

The Ag-Ba-O film exhibited a four-photon emission effect under the influence of the 1.06- μm laser beam, as shown in Figure 3. The Ag-Ba-O film is a novel optoelectronic-conversion film with ultrafine metal particles embedded in a semiconductor substrate. It does not contain any alkali metal and it is fairly stable. It can be stored in the atmosphere and then placed in vacuum to emit sufficient photoelectrons for the detection of picosecond laser pulses without further activation. This optoelectronic-conversion film should have bright prospects in the future.

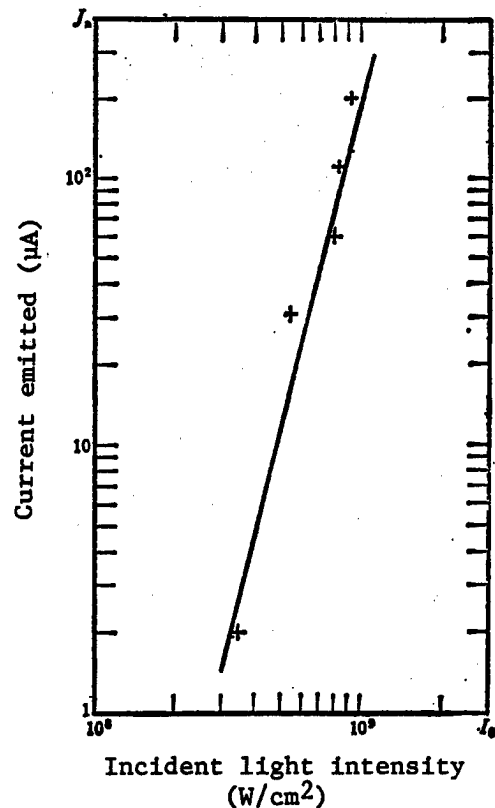


Figure 3. Log J vs. Log I Curve for Multi-Photon Emission ($n = 4$)

References

1. A. H. Sommer, "Photoemissive Materials—Preparation, Properties and Uses," John Wiley & Sons, Inc., 1968.
2. F. Gex et al., Proc. 16th ICHSPP, 1984, p 276.
3. Hayashi Chikara, J. VAC. SCI. TECHNOL., Vol A5, No 4, 1987, p 1375.
4. Li Rulin [2621 1172 2651] et al., WULI [PHYSICS], Vol 17, No 3, 1988, p 133.
5. Wu Quande, Dong Yinwu, and Wu Jinlei, ZHENKONG KEXUE YU JISHU [VACUUM SCIENCE AND TECHNOLOGY], Vol 9, No 4, 1989, p 243.
6. M. Ya. Schelev, SPIE, Vol 384, 1982, p 75.

Optical Implementation of Perfect Shuffle/Exchange Omega Interconnection Network

93FE0536A Shanghai GUANGXUE XUEBAO [ACTA OPTICA SINICA] in Chinese Vol 12 No 12, Dec 92 pp 1129-1134

[Article by Cao Mingcui [2580 2494 5050], Li Hongpu [2621 3163 6225], Luo Fengguang [5012 7364 0342], and Liang Lechu [2733 2867 0443] of the Laser Institute of Huazhong (Central China) University of Science and Technology, Wuhan: "Optical Implementation of Perfect Shuffle/Exchange Omega Interconnection Network"; MS received 17 Oct 91, revised 24 Feb 92, supported by the 863 High-Tech Fund and the National Defense Science, Technology and Industry Commission Research Fund]

[Text] Abstract

An equivalent Omega network comprised of left and right perfect-shuffle interconnections and a spatial optical switch is presented. An optical combination prism with low loss and equal optical path for all channels has been successfully designed to implement perfect shuffle interconnection. A perfect shuffle/exchange interconnection network is realized by using an optical system comprised of two such optical combination prisms and a spatial optical switching array. This optical interconnection network has been experimentally validated.

1. Introduction

The advantage of optical computing is to rely on special characteristics of light, such as high density and freedom from electromagnetic interference, to eliminate inherent disadvantages of electronic computers caused by "wired connection," including bottleneck, crosstalk and clock distortion, in the development of novel parallel, high-data-flow, non-Von Neumann-architecture computers.¹ A

digital optical computer is composed of two-dimensional optical logic connected by an optical interconnection network capable of executing parallel data-flow operations, an optical switching array, and storage devices. Therefore, one of the most important subjects in optical computer research is the optical interconnection network.²

In recent years, free-space optical interconnection networks, such as the shuffle/exchange, crossover and Banyan networks, have attracted considerable attention.³⁻⁵ One of the major reasons is that these optical interconnection networks not only can implement high-speed real-time, parallel, pipelined computations—which is extremely critical to the development of algorithms and architectures for pure optical computing—but also are necessary for the development of hybrid parallel mainframe and optical communication switching systems.⁶ Another important reason is that this type of network, in most cases, is an optical multi-stage interconnection network (MIN). When the number of interconnections is very large, the space-bandwidth product needs to be low and the fan-in and fan-out are 2. Low-loss interconnection between stages can be realized using a polarized prism.

A perfect shuffle/exchange (P.S.) Omega network, or an Omega network, is a free-space regular interconnection network. For parallel, pipelined digital computing, it is capable of implementing a variety of algebraic operations, ordering operations, fast Fourier transformations and matrix operations.⁷ In a parallel, multiprocessor mainframe computer, it is used to interconnect processors, or processors to memories.⁸⁻¹⁰ An Omega interconnection network is an optical network comprised of P.S. element arrays. Several detailed studies have been conducted on P.S. interconnection networks.¹¹⁻¹⁴ However, the optics are more complex and the light energy loss is high. A novel optical method is presented to implement an Omega MIN and it is experimentally validated.

2. Optical P.S. Omega Interconnection Network

The P.S. Omega interconnection network is comprised of an array of perfect-shuffle interconnects and switching elements, as shown in Figure 1.¹⁵ In the figure 01234567 are the inputs and 0'1'2'3'4'5'6'7' are the outputs. P.S. is the perfect shuffle interconnection, and ABCDEFGH are the switching elements. Since it is very difficult to develop an automatic optical channel exchanger, and since the performance of spatial optical switching arrays is close to commercial use, an effective P.S. Omega MIN comprised of left and right P.S. interconnects and spatial light switching arrays has been designed and is presented here in Figure 2. The dotted lines shown in the figure are left P.S. interconnects, the solid lines are right P.S. interconnects, and ABCD is the spatial light switching array. At the output end, each port is interconnected to two specific exchange ports at the input end. The optical channel is controlled by the spatial light switch at all times.

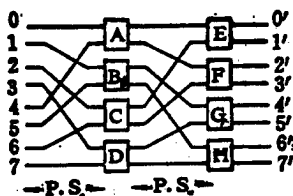


Figure 1. Perfect Shuffle/Exchange Omega Interconnection Network

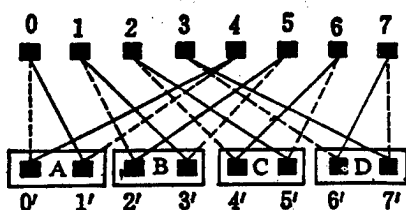


Figure 2. Equivalent Omega Network Consists of Left, Right Perfect Shuffle Interconnects and Spatial Light Switching Device

The mathematical expressions for the left and right P.S. of a one-dimensional array with an even number of N ports at the input and output are:

$$K' = \begin{cases} 2K, & 0 < K < (N/2) \\ 2K - N + 1, & (N/2) < K < N \end{cases} \quad (1)$$

$$K' = \begin{cases} 2K + 1, & 0 < K < (N/2) \\ 2K - N, & (N/2) < K < N \end{cases} \quad (2)$$

where K is the input port number, e.g., 0, 1, 2, ..., (N-1), and K' is the output port number, e.g., 0', 1', 2', ..., (N-1)'. When the input port number and output port number are 8, the left P.S. interconnection described by equation (1) is as shown in Figure 3. Figure 4 shows the right P.S. interconnection described in equation (2). In order to implement optical P.S. interconnection, the authors have developed a prism combination, comprised of a 45° right-angle prism P₁ and a polarizing prism BS₁, as shown in Figure 5. If the input light is p-polarized, the light entering channels 0, 1, ..., [(N/1)-1] passes through the 45° right-angle prism P₁ and the light entering channels (N/2), ..., (N-1) passes through the polarizing prism (with a half-wavelength plate in front of the polarizing prism) to rotate the plane of polarization by 90° and to turn the polarization from p to s. By adjusting the position of P₁ relative to BS₁, channels 0, 1, ..., [(N/2)-1] can be inserted in front of channels (N/2), ...,

(N-1). To make all optical paths equal in length, a high-reflectance optical path compensation mirror C₁ is placed in front of the polarizing prism. This prism combination realizes left and right P.S. The prism combination shown in Figure 6 accomplishes the left and right P.S. interconnection shown in Figure 4. The difference from that shown in Figure 5 is in the relative position between the right-angle prism P₂ and the polarizing prism BS₂, where channels 0, 1, ..., [(N/2)-1] are inserted behind channels (N/2), ..., (N-1). In order to be consistent with the experimental optical configuration, the incident light is assumed to be s-polarized. Hence a half-wave plate is placed in front of P₂.

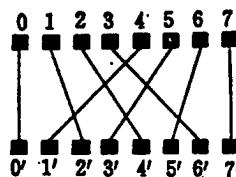


Fig. 3 Left perfect shuffle interconnection network

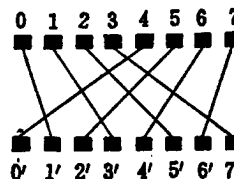


Fig. 4 Right perfect shuffle interconnection network

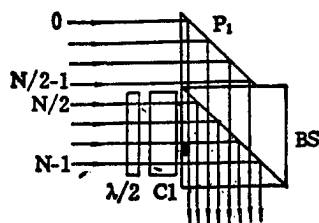


Fig. 5 Optical combination prism of left perfect shuffle interconnection

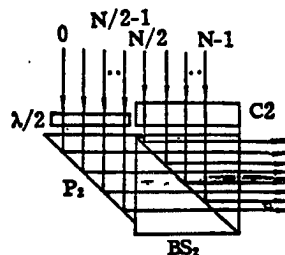


Fig. 6 Optical combination prism of right perfect shuffle interconnection

Figure 7 shows the optical system used to implement the equivalent Omega MIN shown in Figure 2. An 8 x 1 laser beam array passes through a quarter-wave plate to enter the polarizing prism BS₀. It is split into the P and S beam array. The P array enters the prism combination on the upper-right-hand corner to implement left P.S. The optical configuration is identical to that shown in Figure 5. The S array enters the prism combination on the lower-left corner to implement right P.S., as shown in Figure 6. Polarizing prism BS₃ on the lower right combines the left and right P.S. output beam arrays in sequence. The output goes out in two directions. Assume the light beam array on the right is the output. Each port at the output end is interconnected with two switches at the input end. As shown in Figure 2, output ports 0' and 1' are interconnected with input ports 0 and 4. Output ports 2' and 3', 4' and 5', and 6' and 7' are interconnected with input ports 1 and 5, 2 and 6, and 3 and 7, respectively. Furthermore, the optical information channel is controlled by various elements of spatial light switches M₁ and M₂.

3. Experimental Results

In the experiment, a parallel plane film beam splitter is used to split an Ar-ion laser beam into an 8 x 2 array. The lower row is used to mark the input ports; i.e., A, B, C, D, E, F, G and H represent input ports 0, 1, 2, 3, 4, 5, 6 and 7, respectively, as shown in Figure 8 [photograph not reproduced]. Liquid crystal spatial light switches M₁ and M₂ are used to open or close the optical path. The property of the liquid crystal used in the experiment is that it is capable of rotating the polarization of the light beam by 90° when the voltage applied to the liquid crystal is 0; this changes p to s or s to p. When the voltage applied to the pixel is 1, the polarization remains unchanged. In the optical Omega MIN shown in Figure 7, when the voltages on pixels E, A, F, B, G, C, H and D of the spatial light switch M₂ are 1, 0, 1, 0, 1, 0,

1 and 0, respectively, and the voltages on pixels A, E, B, F, C, G, D and H of spatial light switch M₁ are 0, 1, 0, 1, 0, 1, 0 and 1, respectively, the output beam array from the prism combination on the lower-left corner becomes s-polarized after it is modulated by the spatial light switch M₂. After passing the polarizing prism BS₃, all optical channels are cut off to point downward. The beam array in the prism combination on the upper-right corner is converted to s-polarized light after passing through the spatial light modulating switch M₁. Upon entering the polarizing prism BS₃, all optical channels are turned toward the right and exit from the output end. The output array of the Omega MIN is A, E, B, F, C, G, D and H, as shown in Figure 9 [photograph not reproduced], and left P.S. is implemented. When the voltages of the pixels of M₂ are 0, 1, 0, 1, 0, 1, 0, 1, and the voltages of the pixels of M₁ 1, 0, 1, 0, 1, 0, 1, 0, the output channels from the prism combination on the upper-right corner are deflected downward. The output of the optical channels of the prism combination on the lower-left corner are opened to allow light to leave from the output end. Therefore, the output array of the Omega MIN is E, A, F, B, G, C, H and D, as shown in Figure 10 [photograph not reproduced], and right P.S. is accomplished. If output ports 0', 1', and 4', 5', are interconnected to input ports 0, 4 and 2, 6 at one moment and then to 4, 0 and 6, 2 at another, then it is necessary to adjust the voltages of pixels A, E, C, G of M₁ and E, A, G, C of M₂ just before executing an operation. For instance, if the voltages of the pixels in M₁ are 0, 1, 1, 0, 0, 1, 1, 0 and those of M₂ are 1, 0, 0, 1, 1, 0, 0, 1, then the output beam array of the optical Omega MIN is A, E, F, B, C, G, H, D, as shown in Figure 11 [photograph not reproduced]. Compared to Figure 10, the interconnection between output ports 0', 1' and 4', 5' to input ports 0, 4 and 2, 6 can be exchanged by controlling the voltages applied to the pixels of M₁ and M₂. Other output ports can perform exchanges with the two pairs of corresponding input ports, as shown in Figure 2.

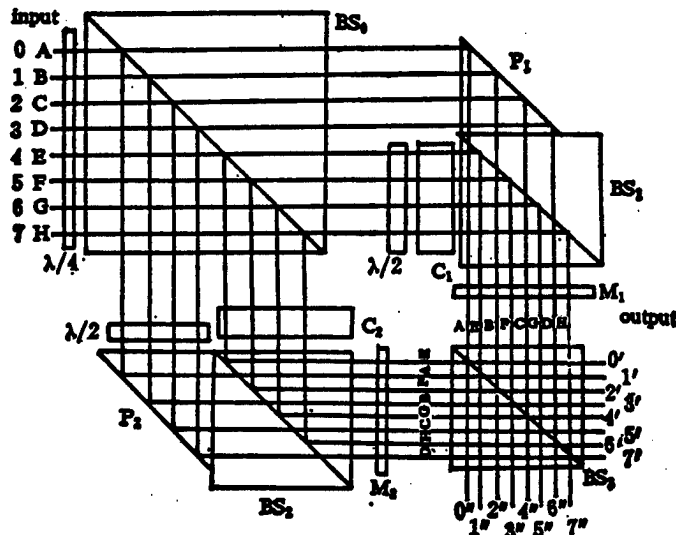


Figure 7. The Optical System of Perfect Shuffle/Exchange Omega Interconnection Network

4. Discussion and Conclusions

A P.S. Omega network is a very important MIN for parallel, pipelined digital optical computers, hybrid optoelectronic massively parallel and multi-processor computers, and optical communication switching networks. An equivalent Omega network is presented in this paper and an optical Omega MIN comprised of two P.S. combination prisms and liquid-crystal spatial light switching arrays has been tested. This interconnection network has characteristics such as simplicity, equal path length, low loss and modular structure. The system has two output ends, one to output results and the other to feedback information. It is particularly suited for optical parallel, pipelined digital computers. It significantly simplifies the hardware in the system. This MIN is a proof-of-principle experiment to optically implement an Omega network. The density and transfer time of an optical MIN are primarily determined by the 1-10 micron micro-optical devices currently under development, such as the surface-emitting laser array,¹⁶ microlens array,¹⁷ and micro-staircase telescope array,¹⁸ as well as by interconnects such as the high-speed spatial light switching array and optically bistable S-SEED logic switching array.¹⁹ The development of these devices creates excellent conditions for perfecting high-density parallel beam arrays and multi-purpose modular interconnects. In the proposed network, the light source can be replaced by a high-density parallel beam array and the liquid-crystal spatial light switch can be replaced by a high-speed ferroelectric liquid crystal switch or other kind of spatial light switch. The simple, equal-path-length, low-loss MIN can be developed into a multi-purpose, programmable, modular micro-interconnection network device.

References

1. A. Huang, "Parallel Algorithms for Optical Digital Computers," New York: Tenth International Optical Computing, IEEE Computer Society, 1983: 13-17.
2. M. E. Prise, N. Streibl, M. M. Downs, "Optical Considerations in the Design of a Digital Computer," *OPT. QUANTUM ELECTRON.*, 1988, 20 (1): 49-77.
3. K. H. Brenner, A. Huang, N. Streibl, "Digital Optical Computing With Symbolic Substitution," *APPL. OPT.*, 1986, 25 (18): 3054-3060.
4. M. J. Murdocca, A. Huang, J. Jahns, et al., "Optical Design of Programmable Logic Arrays," *APPL. OPT.*, 1988, 27 (9): 1651-1660.
5. J. Jahns, M. J. Murdocca, "Crossover Networks and Their Optical Implementation," *APPL. OPT.*, 1988, 27 (15): 3155-3160.
6. M. Murdocca, T. J. Cloonan, "Optical Design of a Digital Switch," *APPL. OPT.*, 1989, 28 (13): 2505-2517.
7. T. Lang, H. S. Stone, "A Shuffle-Exchange Network With Simplified Control," *IEEE TRANS. COMPUT.*, 1976, C-25 (1): 55-65.
8. T. Lang, "Interconnections Between Processors and Memory Modules Using the Shuffle-Exchange Network," *IEEE TRANS. COMPUT.*, 1976, C-25 (5): 496-503.
9. D. H. Lawrie, "Access and Alignment of Data in an Array Processor," *IEEE TRANS. COMPUT.*, 1975, C-24 (12): 1145-1155.
10. C. Wu, T. Feng, "The Universality of the Shuffle-Exchange Network," *IEEE TRANS. COMPUT.*, 1981, C-30 (5): 324-332.
11. M. T. Tsao, H. P. Li, X. A. Liu, "Optical Hardware for the Perfect Shuffle Interconnection," *OPTICAL COMPUTING AND PROCESSING*, 1991, 1 (1): 23-27.
12. J. W. Goodman, J. F. Leonberger, S. Y. Kung, et al., "Optical Interconnections for VLSI System," *PROC. IEEE*, 1984, 72: 850.
13. A. W. Lohmann, S. Stork, G. Syucke, "Optical Perfect Shuffle," *APPL. OPT.*, 1986, 25 (9): 1530.
14. K. H. Brenner, A. Huang, "Optical Implementations of Perfect Shuffle Interconnection," *APPL. OPT.*, 1988, 27 (1): 135-137.
15. C. Wu, T. Feng, "On a Class of Multistage Interconnection Networks," *IEEE TRANS. COMPUT.*, 1980, C-29 (8): 694-702.
16. Y. H. Lee, J. L. Jewell, A. Scherer, et al., "Room-Temperature Continuous-Wave Vertical Cavity Single Quantum Well-Microlaser Diodes," *ELECTRON. LETT.*, 1989, 25 (20): 1377-1378.
17. D. Barahowski, L. G. Mann, R. H. Bellman, et al., "Photothermal Technique Generates Lens Arrays," *LASER FOCUS WORLD*, 1989, 25 (11): 139-143.
18. A. W. Lohman, F. Sauer, "Staircase Telescope Arrays for Local Beam Compression in One Dimension," *APPL. OPT.*, 1989, 28 (18): 3830.
19. D. A. B. Miller, J. E. Henry, A. C. Gossard, et al., "Integrated Quantum Well Self Electro-Optic Effect Device: 2 x 2 Array of Optically Bistable Switches," *APPL. PHYS. LETT.*, 1986, 49: 821-823.

Carrier-Injected GaAs/GaAlAs Total Internal Reflection Optical Switch

93FE0536B Beijing BANDAOTI XUEBAO [CHINESE JOURNAL OF SEMICONDUCTORS] in Chinese Vol 14 No 1, Jan 93 pp 1-5

[Article by Zhuang Wanru [8369 1238 1172], Lin Wenhua [2651 7186 5478], Yang Peisheng [2799 1014 3932], Li Ren [2621 0117], Shi Zhiwen [4258 1807 2429], Zhao Yibing [6392 0001 0365], Sun Furong [1327 1431 2837], Gao Junhua [7559 0193 5478], and Liu Tao [0491 3447] of the National Integrated Optoelectronics Laboratory of the Institute of Semiconductors of the Chinese Academy of Sciences, Beijing 100083: "Carrier-Injected GaAs/GaAlAs Total-Internal-Reflection Optical Switch"; MS received 4 Nov 91, revised 11 Feb 92]

[Text] Abstract

A carrier-injected (CI) band-filling-effect total internal reflection (TIR) GaAs/GaAlAs optical waveguide switch has been developed. The operating wavelength of the switch is 0.87 μm , operating current is 70 mA, the extinction ratio is 14 dB and the crosstalk is -13 dB. This switch has advantages such as small size, independence of polarization, non-blocking and ease of monolithic integration.

I. Introduction

The optical waveguide switching array is an important component in fiber-optic communication switching systems and optical information processing systems. Particularly, it is a key component in broadband optical switching network technology. In the past, LiNbO_3 has been the primary material for an optical waveguide switch. In recent years, because of the need in optoelectronic integration and optical integration, development of optical waveguide switches made of III-V compound semiconductors has progressed very rapidly. These switches play a vital role in the miniaturization, integration and commercialization of various systems. Semiconductor optical waveguide switches can be classified into two types, i.e., DC¹⁻² (directional coupling) and TIR³ (total internal reflection) switches. The TIR switch is small and involves less technical risks; it is easier to monolithically integrate with an active semiconductor device. Moreover, it is easier to fabricate it into a large N x N switching array.

The TIR switch requires a relatively large refractivity change. The CI band-filling effect just happens to be able to produce a large refractivity change Δn . When the injected carrier density is greater than 10^{18} cm^{-3} , Δn can be as high as 1×10^{-2} , which is two orders of magnitude higher than the change produced by optoelectronic effects. Furthermore, it is independent of the polarization of the incident light.⁴ These properties happen to meet the requirements for a TIR switch. Therefore, fabrication of TIR semiconductor optical waveguide switches based on CI band-filling effect is a new development trend worldwide.⁴⁻⁵

The design, fabrication and experimental results of a novel GaAs/GaAlAs heterojunction CI-TIR switch are described for the first time in this paper.

II. Principle and Design of the CI-TIR Switch

Figures 1(a) and 1(b) show the principle of the GaAs/GaAlAs CI-TIR switch. Two single-mode waveguides are crossed to form an angle θ . A PIN [positive-intrinsic-negative] structure is formed in the overlapping area by means of Zn diffusion. When the device is positively biased by injection of electrons and holes, the refractivity in the CI zone decreases substantially due to the band-filling effect. If the incident light enters at an angle greater than the critical angle, TIR occurs at the interface where the refractivity drops to alter the optical path. The light leaves from the reflected end to produce the optical switching effect.

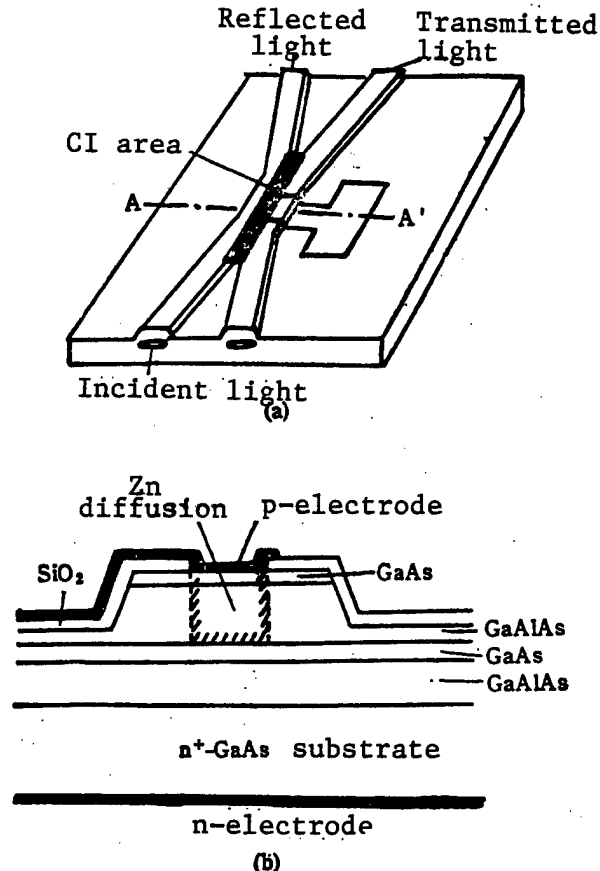


Figure 1. GaAs/GaAlAs CI-TIR Optical Waveguide Switch
(a) Structure; (b) Structure of AA' Cross Section

When the number of carriers injected reaches a certain level, the electron quasi-Fermi level, E_{FN} , is a few kT in the conduction band and the hole quasi-Fermi level, E_{FP} , is also a few kT in the valence band; this results in the

band-filling effect. The outcome is a shift in the absorption edge toward higher energy (i.e., blue shift). Based on the Kramers-Kronig formula, the change of refractivity, Δn , caused by the band-filling effect is:⁶

$$\Delta n(\Delta N, \Delta P, E) = \frac{c\hbar}{\epsilon^2} P \int_0^\infty \frac{\Delta \alpha(\Delta N, \Delta P, E')}{E'^2 - E^2} dE', \quad (1)$$

where ΔN is the number of electrons injected, ΔP is the number of holes injected, $\Delta \alpha$ is the change of absorption coefficient, E represents the incident photon energy, and $P[\text{integral}]$ represents a principal-value integration. Figure 2 shows a family of Δn dispersion curves corresponding to different concentrations injected into GaAs. From the figure, Δn falls most in the bandgap. Considering the fact that the bandgap is very close to the absorption edge, the absorption loss is high. To this end, the waveguide needs to be shifted toward higher energy to 50-100 meV.

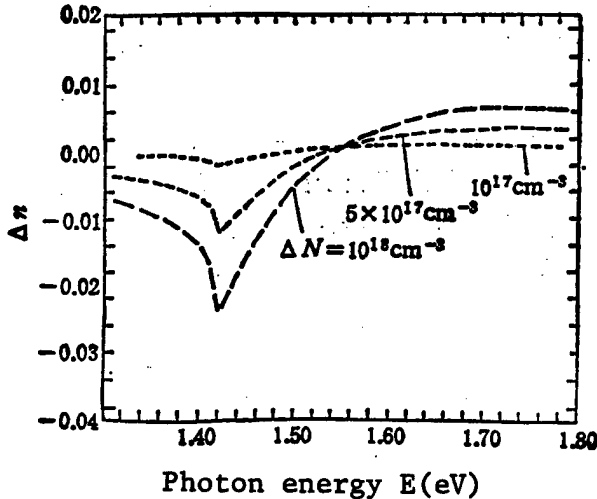


Figure 2. Dispersion of Refractivity Change in GaAs Caused by Band-Filling

A heterojunction structure is employed for the CI-TIR switch to limit the injected electrons and holes in the waveguide layer in order to make it easy to raise the injected carrier concentration. The change of refractivity caused by band-filling, Δn , increases linearly with the injected carrier concentration ΔN . For single-crystal GaAs, numerical computation shows that:⁷

$$\begin{aligned} \Delta n &= -2.2 \times 10^{-20} \Delta N & (E = 1.40 \text{ eV}) \\ &= -1.7 \times 10^{-20} \Delta N & (E = 1.37 \text{ eV}) \\ &= -1.5 \times 10^{-20} \Delta N & (E = 1.36 \text{ eV}) \\ &= -1.0 \times 10^{-20} \Delta N & (E = 1.32 \text{ eV}) \end{aligned} \quad (2)$$

When ΔN falls in the 10^{16} - 10^{18} cm^{-3} range, there is excellent agreement between experimental results and the calculated values shown above. However, when ΔN is above 10^{19} cm^{-3} , the Δn to ΔN relationship becomes

quasi-linear. It is also influenced by other effects. When the injected carrier concentration is 10^{18} cm^{-3} , the magnitude of refractivity change can be as high as 10^{-2} . The injected carrier concentration is given as follows:

$$\Delta N = J\tau/qd, \quad (3)$$

where J is the injected current density, τ is the injected carrier lifetime, and d is the thickness of the waveguide layer.

When TIR occurs, the critical angle θ_c is:

$$\theta_c = \sin^{-1} (1 + \Delta n/n_w) \quad (4)$$

where n_w is the refractivity of the waveguide layer.

The modeling of a 2 x 2 CI-TIR switch array has been done in reference 8. Correlation curves between extinction ratio, crosstalk and reflection loss as a function of structural parameters of the switch have been obtained. The effect of refractivity change caused by different injected carrier levels on the performance of the switch and the effect of the waveguide absorption coefficient on its performance are also determined. These curves may be used to optimize the design of CI-TIR switches.

The longitudinal cross section of a CI-TIR switch is shown in Figure 1(b). Two 4- μm -wide heterojunction GaAs/GaAlAs waveguides are crossed at an angle θ . Although the smaller θ is, the closer the reflectance approaches 1, when $\theta/2 < 1^\circ$, waveguide modes interact with each other, which enhances crosstalk. Therefore, θ was chosen to be 4° . The overlapping area is 90 μm long and 4 μm wide. The radius of the curved waveguide is 2 mm and the distance between the ends of the two waveguides is 50 μm .

The following layers are grown on top of the n^+ -GaAs substrate by liquid phase epitaxy: an n^+ -GaAs buffer layer, an $\text{N-Ga}_{0.7}\text{Al}_{0.3}\text{As}$ lower confinement layer, an un-doped $\text{Ga}_{0.94}\text{Al}_{0.06}\text{As}$ waveguide layer, an un-doped $\text{Ga}_{0.7}\text{Al}_{0.3}\text{As}$ upper confinement layer, and a GaAs top layer. The bandgap wavelength of the waveguide layer is 0.82 μm . The substrate concentration is $< 1 \times 10^{17} \text{ cm}^{-3}$ and substrate thickness is 0.5 μm . A 1.0- μm -high mesa carrier waveguide is fabricated by reactive ion etching (RIE). A p-i-n junction is formed at the overlapping center area by means of Zn diffusion. The Cr/Au pattern of the p electrode is prepared by stripping. The n electrode is made of an Au/Ge/Ni alloy. The wafer is then cleaved into chips. Each device is 1 mm in length and 340 μm in width. Figure 3(a) [photograph not reproduced] is a picture of the CI-TIR chip sintered on a heat sink. Figure 3(b) [photograph not reproduced] is a picture of the end view of the chip.

III. Performance Measurement and Discussion

The CI-TIR switch is measured using a 0.87- μm GaAs/GaAlAs laser with a single-mode fiber pigtail as the light source. An infrared camera is used to obtain the near-field pattern at its output. It is scanned with a selector

and the output light-spot mode-field distribution is recorded with an oscilloscope.

The n-term static parameters of the CI-TIR switch are defined as follows:

transmissive-end extinction ratio: $E_t = 10 \log I_t(0)/I_t(I)$

reflective-end extinction ratio: $E_r = 10 \log I_r(I)/I_r(0)$

where $I_t(0)$ and $I_t(I)$ represent the output intensities at the transmissive end when $\Delta n = 0$ (i.e., without current injected) and $\Delta n < 0$ (i.e., with injected current), respectively. $I_r(0)$ and $I_r(I)$ represent the output intensities at the reflective end when $\Delta n = 0$ and $\Delta n < 0$, respectively.

crosstalk when closed (without injected current): $CT(0) = 10 \log I_r(0)/I_t(0)$

crosstalk when open (with injected current): $CT(I) = 10 \log I_t(I)/I_r(I)$

overall insertion loss of the switch: $L_t = 10 \log I_t/I_t(0)$

where I_t is the light intensity at the input.

When the incident wavelength is $0.87 \mu\text{m}$, the output at the transmissive end, I_t , decreases as the injected current increases and the output at the reflective end, I_r , gradually increases. For device #25, when the injected current is 60 mA (i.e., equivalent to a current density of 6.6 kA/cm^2), most light comes out of the reflective end. Optical switching is thus accomplished. Figure 4 [photograph not reproduced] shows a picture of the near field of the spot and a recording of the optical field distribution.

Figure 5 shows how normalized I_t and I_r vary as a function of injected current for switch #19. As the injected current increases, I_t gradually falls and I_r gradually rises. The total optical power output ($I_t + I_r$), however, does not drop much as a function of injected current. This indicates that the CI-TIR switch does not create a substantial loss when switching from an open to a closed state. With an injected current of 70 mA, the extinction ratio at the transmissive end, E_t , was measured to be 14 dB; the extinction ratio at the reflective end, E_r , was 19 dB. The crosstalk when the switch is open is -13 dB and that when the switch is closed is -20 dB.

The transmissive waveguide was chosen to measure the loss of the CI-TIR switch and the total insertion loss was determined to be 14.3 dB. This includes 4-5 dB of coupling loss between the optical fiber and the switch, a 3-dB reflective loss at both ends, and a 1-2 dB loss each due to bending and scattering. Based on this data, the transmission loss of the waveguide is estimated to be about 1 dB/mm.

Since the primary function of the CI-TIR switch is to perform switch conversion in an optical switching

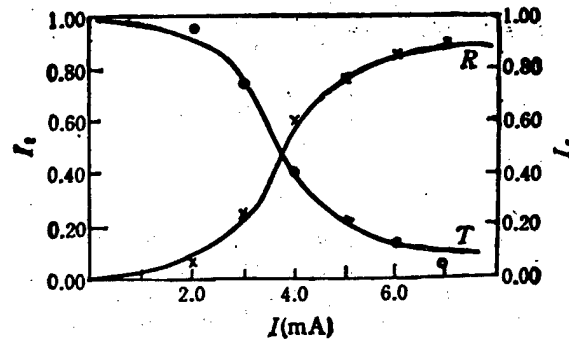


Figure 5. I_t and I_r of the #19 CI-TIR Switch as a Function of Injected Current

network and it is not being used in any high-speed systems, dynamic characteristics such as high-speed modulation have not been measured. By substituting the static results into equations (1)-(4), we know that switching can only be accomplished when the carrier concentration exceeds 10^{18} cm^{-3} (i.e., Δn needs to be of the order of 10^{-2}). The key to having an excellent device is to ensure a smooth interface for the region of varying refractivity. Furthermore, the impurity concentration of the substrate needs to be lowered to improve various properties of the device. The next step is to use MOCVD to epitaxially grow the heterojunction structure in order to lower the impurity level of the substrate to 10^{15} cm^{-3} and thereby further improve the switching current and transmission loss.

IV. Conclusion

A novel TIR GaAs/GaAlAs heterojunction optical waveguide switch has been developed. It uses the band-filling effect caused by CI to produce a relatively large change of refractivity to realize switching. Experimental results are found to be in excellent agreement with theoretical analysis. Since carrier injection is isotropic, the CI-TIR switch is polarization-independent. The switching electrodes are symmetrically placed in the middle of the overlapping area. The device can be made into a non-blocking 2×2 switching unit. This switching unit can be made into a switch array for an optical switching system. This switch array is small and has a heterojunction structure similar to that of active semiconductor devices. It is technically compatible with OEIC and PIC [photonic integrated circuit] technology and can easily be integrated with optoelectronic devices on the same chip.

Acknowledgment

The authors wish to express their sincere gratitude toward Zhu Longde [2612 7893 1795] and Jin Caizheng [6855 2088 2398] for providing key test equipment to allow the work to proceed smoothly.

References

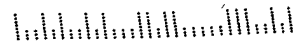
1. J. C. Cambell, et al., APPL. PHYS. LETT., Vol 27, 1975, p 202.
2. A. Carencio, et al., APPL. PHYS. LETT., Vol 40, 1982, p 15.
3. C. S. Tsai, et al., IEEE J. QUANTUM ELECTRONICS, Vol QE-14, 1978, p 513.
4. H. Inoue, et al., IEEE J. SELECTED AREAS IN COMMUNICATION, Vol 6, 1988, p 1262.
5. M. Renaud, et al., ECOC'90, p 217.
6. B. R. Bennett, et al., IEEE J. QUANTUM ELECTRONICS, Vol 26, No 1, 1990, p 113.
7. Lin Wenhua, Wang Dehuang [3769 1795 3552], and Zhuang Wanru, Proceedings of the 1991 Annual Conference on Optoelectronic Devices and Integration Technology, 1991.
8. Lin Wenhua, Zhuang Wanru, and Wang Dehuang, BANDAOTI XUEBAO [CHINESE JOURNAL OF SEMICONDUCTORS], 1993, to be published.
9. S. H. Lin, et al., ELECTRONICS LETT., Vol 21, 1985, p 597.

NTIS
ATTN PROCESS 103
5285 PORT ROYAL RD
SPRINGFIELD VA

2

22161

BULK RATE
U.S. POSTAGE
PAID
PERMIT NO. 352
MERRIFIELD, VA.



This is a U.S. Government publication. Its contents in no way represent the policies, views, or attitudes of the U.S. Government. Users of this publication may cite FBIS or JPRS provided they do so in a manner clearly identifying them as the secondary source.

Foreign Broadcast Information Service (FBIS) and Joint Publications Research Service (JPRS) publications contain political, military, economic, environmental, and sociological news, commentary, and other information, as well as scientific and technical data and reports. All information has been obtained from foreign radio and television broadcasts, news agency transmissions, newspapers, books, and periodicals. Items generally are processed from the first or best available sources. It should not be inferred that they have been disseminated only in the medium, in the language, or to the area indicated. Items from foreign language sources are translated; those from English-language sources are transcribed. Except for excluding certain diacritics, FBIS renders personal names and place-names in accordance with the romanization systems approved for U.S. Government publications by the U.S. Board of Geographic Names.

Headlines, editorial reports, and material enclosed in brackets [] are supplied by FBIS/JPRS. Processing indicators such as [Text] or [Excerpts] in the first line of each item indicate how the information was processed from the original. Unfamiliar names rendered phonetically are enclosed in parentheses. Words or names preceded by a question mark and enclosed in parentheses were not clear from the original source but have been supplied as appropriate to the context. Other unattributed parenthetical notes within the body of an item originate with the source. Times within items are as given by the source. Passages in boldface or italics are as published.

SUBSCRIPTION/PROCUREMENT INFORMATION

The FBIS DAILY REPORT contains current news and information and is published Monday through Friday in eight volumes: China, East Europe, Central Eurasia, East Asia, Near East & South Asia, Sub-Saharan Africa, Latin America, and West Europe. Supplements to the DAILY REPORTs may also be available periodically and will be distributed to regular DAILY REPORT subscribers. JPRS publications, which include approximately 50 regional, worldwide, and topical reports, generally contain less time-sensitive information and are published periodically.

Current DAILY REPORTs and JPRS publications are listed in *Government Reports Announcements* issued semimonthly by the National Technical Information Service (NTIS), 5285 Port Royal Road, Springfield, Virginia 22161 and the *Monthly Catalog of U.S. Government Publications* issued by the Superintendent of Documents, U.S. Government Printing Office, Washington, D.C. 20402.

The public may subscribe to either hardcover or microfiche versions of the DAILY REPORTs and JPRS publications through NTIS at the above address or by calling (703) 487-4630. Subscription rates will be

provided by NTIS upon request. Subscriptions are available outside the United States from NTIS or appointed foreign dealers. New subscribers should expect a 30-day delay in receipt of the first issue.

U.S. Government offices may obtain subscriptions to the DAILY REPORTs or JPRS publications (hardcover or microfiche) at no charge through their sponsoring organizations. For additional information or assistance, call FBIS, (202) 338-6735, or write to P.O. Box 2604, Washington, D.C. 20013. Department of Defense consumers are required to submit requests through appropriate command validation channels to DIA, RTS-2C, Washington, D.C. 20301. (Telephone: (202) 373-3771, Autovon: 243-3771.)

Back issues or single copies of the DAILY REPORTs and JPRS publications are not available. Both the DAILY REPORTs and the JPRS publications are on file for public reference at the Library of Congress and at many Federal Depository Libraries. Reference copies may also be seen at many public and university libraries throughout the United States.